Kaunas University of Technology

Faculty of Mathematics and Natural Sciences

Effects of Alpha Particles on Cells

Master's Final Degree Project

Džiugilė Valiukevičiūtė

Project author

Prof. Dr. Diana Adlienė

Supervisor

Dr. Jonas Venius

Consultant, National Cancer Institute

Kaunas, 2024

Kaunas University of Technology

Faculty of Mathematics and Natural Sciences

Effects of Alpha Particles on Cells

Master's Final Degree Project

Medical Physics (6213GX001)

Džiugilė Valiukevičiūtė

Project author

Prof. Dr. Diana Adlienė

Supervisor

Dr. Jonas Venius

Consultant, National Cancer Institute

Prof. Dr. Giedrius Laukaitis

Reviewer

Kaunas, 2024

Kaunas University of Technology

Faculty of Mathematics and Natural Sciences

Džiugilė Valiukevičiūtė

Effects of Alpha Particles on Cells

Declaration of Academic Integrity

I confirm the following:

1. I have prepared the final degree project independently and honestly without any violations of the copyrights or other rights of others, following the provisions of the Law on Copyrights and Related Rights of the Republic of Lithuania, the Regulations on the Management and Transfer of Intellectual Property of Kaunas University of Technology (hereinafter – University) and the ethical requirements stipulated by the Code of Academic Ethics of the University;

2. All the data and research results provided in the final degree project are correct and obtained legally; none of the parts of this project are plagiarised from any printed or electronic sources; all the quotations and references provided in the text of the final degree project are indicated in the list of references;

3. I have not paid anyone any monetary funds for the final degree project or the parts thereof unless required by the law;

4. I understand that in the case of any discovery of the fact of dishonesty or violation of any rights of others, the academic penalties will be imposed on me under the procedure applied at the University; I will be expelled from the University and my final degree project can be submitted to the Office of the Ombudsperson for Academic Ethics and Procedures in the examination of a possible violation of academic ethics.

Džiugilė Valiukevičiūtė

Confirmed electronically

Valiukevičiūtė, Džiugilė. Effects Of Alpha Particles On Cells. Master's Final Degree Project / supervisor prof. dr. Diana Adlienė, Faculty of Mathematics and Natural Sciences, Kaunas University of Technology; consultant dr. Jonas Venius, National Cancer Institute.

Study field and area (study field group): Medical Technologies (Health Sciences).

Keywords: alpha particles, spheroids, glioblastoma, prostate cancer, ^{223}Ra.

Kaunas, 2024. 62 p.

Summary

Targeted alpha therapy (TAT) shows promising results for precise and selective radiotherapy with effective cancer treatment and minimal toxicity. Alpha particle emitters are linked to the targeted molecules for the selective delivery of ionizing radiation to the malignant cells, and due to the short path length (~65 µm), only a few cells are affected. A short distance of irradiation ensures minimal toxicity for the healthy cells around and provides the possibility to treat very small targets—groups of cells. In combination with less selective treatments, targeted alpha therapy could provide higher treatment quality with a decreased probability of cancer recurrence. However, targeting agents, dose regiments, and possible alpha particle emitters raise questions that should be answered.

This project aimed to evaluate the effect of different doses of alpha (^{223}Ra) and gamma (6 MeV photons) radiation on the size and viability of glioblastoma and prostate cancer 3D cell cultures and provide recommendations for future experiments. The size of cell structures was evaluated on the 7th and 14th-day post-irradiation, and the effect on viability was analyzed on the 14th day post-irradiation.

It was found that with increased specific activity of the alpha particle emitter ^{223}Ra solution both 3D cell cultures showed a decrease in size. The same effect was observed after irradiation with photons. The viability test showed a significant positive correlation between spheroid size and viability, indicating the possibility of determining spheroid viability from the size measurements.

Valiukevičiūtė, Džiugilė. Alfa dalelių poveikis ląstelėms. Magistro baigiamasis projektas / vadovė prof. dr. Diana Adlienė, Kauno technologijos universitetas, Matematikos ir gamtos mokslų fakultetas; konsultantas dr. Jonas Venius, Nacionalinis vėžio institutas.

Studijų kryptis ir sritis (studijų krypčių grupė): Medicinos technologijos (Sveikatos mokslai).

Reikšminiai žodžiai: alfa dalelės, sferoidai, glioblastoma, prostatos vėžys, ^{223}Ra.

Kaunas, 2024. 62 p.

Santrauka

Tikslinė alfa dalelių terapija gali būti naudojama didelio tikslumo ir selektyvumo radioterapijoje taip sumažinant sveikų audinių pažaidas, bet efektyviai naikinant vėžį. Siekiant selektyviai apšvitinti piktybines ląsteles, spinduliuotės pernešėjai - alfa spinduoliai - yra susiejami su tikslinėmis molekulėmis. Tikslingas energijos transportavimas ir trumpas alfa dalelių skverbimosi atstumas (~65 µm) sąlygoja spinduliuotės poveikį tik keliems ląstelių sluoksniams ir minimalias pažaidas sveikiems audiniams. Įvairių radioterapijos metodų kombinavimas užtikrintų gydymo tikslumą ir sumažintų vėžio atsinaujinimo tikimybę. Pagrindinės problemos, su kuriomis susiduriama taikant tikslinę alfa dalelių terapiją klinikinėje aplinkoje, yra siejamos su galimais selektyvių alfa dalelių nešėjais, alfa dalelių šaltiniais bei gydymui skiriamomis dozėmis.

Šio darbo tikslas įvertinti alfa (^{223}Ra) ir gama (6 MeV) spinduliuotės dozių įtaką glioblastomos ir prostatos vėžio trimačių struktūrų dydžiui ir gyvybingumui, bei pateikti rekomendacijas tolimesniems tyrimams. Spindulinės apšvitos įtaka trimačių struktūrų dydžiui buvo vertinami 7-tą ir 14-tą dieną po apšvitos , o gyvybingumas buvo vertinamas praėjus 14 dienų po apšvitos.

Nustatyta, kad didėjant ^{223}Ra tirpalo savitajam aktyvumui, abiejų 3D ląstelių kultūrų matmenys traukėsi. Ląstelių struktūrų mažėjimas priklausomai nuo sugertos dozės buvo stebimas ir paveikus jas rentgeno spinduliuote. Tarp 3D ląstelių kultūros gyvybingumo ir dydžio pokyčių buvo nustatyta stipri teigiamą koreliacija, todėl siūloma ląstelių struktūros matmenų pokytį naudoti ląstelių gyvybingumui vertinti.

Table of contents

List of figures

List of tables

Introduction

Radiotherapy is one of the most effective therapies for cancer treatment. This method has been used since the discovery of X-rays in 1895 [1]. Due to its high efficiency in killing cancer, radiotherapy has proven its applicability. Despite the benefits of the treatment, conventional radiotherapy also has drawbacks: limited accuracy, toxicity, and limited possibilities to treat very small targets. Nowadays, the focus is on the new generation of radiotherapy, which would allow for more precise, personalized treatment with increased healthy tissue toxicity [2].

Alpha particles have shown promise for personalized and accurate radiotherapy. These particles have a high linear energy transfer, which can cause significant damage to cells. Their short range of penetration, combined with high chelator selectivity, would allow for targeting micrometastases and cell groups. When used in combination with other treatment methods, they can provide a synergistic effect. Despite its benefits, targeted alpha-particle therapy is not widely used in clinical practice. However there is a strong focus on creating highly selective chelator agents, determining dose regimens for the best results in combination with other treatment methods, and developing delivery strategies [3, 4].

Application of cell cultures is a well addopted for *in vitro* studies of biological tissue responses to ionizing radiation. Among various methods, the application of 3D cell cultures stands out as an accurate method to analyze tumor radiobiological responses due to the accurate representation of the tumor microenvironment by the cells [5].

Aim of the work:

Investigation of alpha and gamma irradiation dose on the size and viability of glioblastoma and prostate cancer 3D cell cultures and preparation of recommendations for future investigations.

Tasks of the work:

- to evaluate the influence of ^{223}Ra solution activity on the size of prostate cancer and glioblastoma spheroids;
- to determine the specific activity at which prostate cancer and glioblastoma spheroids size could be reduced by 20%;
- to evaluate the influence of ^{223}Ra solution activity on cell viability using XTT assay and viability correlation with spheroid size;
- to evaluate the influence of irradiation dose of 6 MeV photons on the size of prostate cancer and glioblastoma spheroids;
- to determine the absorbed dose values for spheroids treated with ^{223}Ra solution.

1. Literature review

1.1. Radiobiological mechanisms inside the cell

The ionizing radiation-induced effects on live organisms start at a cellular level. When ionizing radiation (x-rays, gamma rays, or charged particles) interacts with biological tissue, part of the energy is deposited in the tissue, and may cause indirect or direct responses. If ionizing radiation is absorbed in biological material, there is a high possibility that direct interaction will occur with the main target in the cell, DNA (deoxyribonucleic acid) [6]. There is a lot of evidence that radiation-induced cell death is due to changes in its nuclear environment, mainly in the genetic information (DNA), but changes in the nuclear membrane can also contribute to the radiation-induced death of the cell. When ionizing radiation passes through the nucleus of the cell, the atoms of DNA will be excited due to the absorbed energy, which will start the chain of events leading to the biological change [6]. This response to the ionizing radiation is the main one, and it is called the direct action response.

On the other hand, when ionizing radiation energy is absorbed in the cell environment (not in the target), the atoms (in the majority of cases, water molecules) are excited and produce free radicals. Radicals can diffuse and reach critical targets in the cell. Figure 1 represents schematically the direct and indirect responses to ionizing radiation at the molecular level [6, 7].

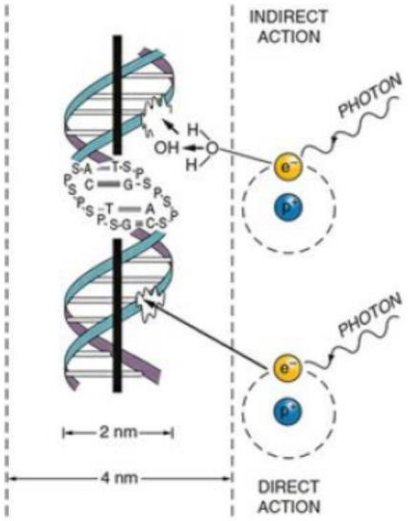

Fig. 1 Indirect and direct actions of ionizing radiation at the molecular level [6].

At this time, there is no doubt that DNA is the most important target to induce radiobiological responses, including cell killing, carcinogenesis, and mutation [6, 7]. All these possible effects depend on the structural changes of DNA. For a deeper understanding of the effects of ionizing radiation, it is important to look closer at the radiation-induced breaks in DNA on the path of charged particles and the action of chemical radicals produced in the cell [6].

1.1.1. Types of DNA damage due to ionizing radiation

The biological effect of ionizing radiation is evaluated by the breaks produced in DNA. DNA is a large molecule with a helix structure. DNA is made from an alternant sugar (deoxyribose), phosphate groups, and four bases (adenine, cytosine, guanine, and thymine). This macromolecule is very

important for the whole organism; it stores genetic information, and even small changes can cause functioning disruption [8].

The damage to the cell could be sub-lethal or lethal. Sub-lethal damage is when the number of DNA damages is small and has the potential to be repaired. Sub-lethal damage is usually caused by low-dose exposure. On the other hand, lethal damage occurs when the damage is irreparable (typical for high exposure doses) [7].

The damage to DNA could be separated into two groups: double-strand breaks (DSB) and single-strand breaks (SSB). SSB‘s damages are easily repaired by the replication of the second strand of DNA, but DSB damages are much more significant since they may lead to radiation-induced cell death. DSB occurs when two single-strand breaks are close or both DNA strands break at the site of interaction. The spatial distribution of DSB is a key factor that could cause cell death. This kind of break could be repaired by two mechanisms: homologous recombination repair (HRR) and nonhomologous end joining (NHEJ). HRR uses the second, undamaged strand of DNA as a template. This repair mechanism is error-free because the sequence of bases is complementary. On the other hand, the NHEJ mechanism is error-prone because no template is used for the reparation. The mechanism that will be used for the reparation is dependent on the phase of the cell cycle [6, 7, 9].

The changes in DNA can introduce apoptotic or mitotic death. The most common death from ionizing radiation is mitotic. This death usually occurs in the first or second division of the cell after exposure; the cell is incapable of finishing mitosis if the damage to DNA is not repaired correctly. This cell-killing mechanism causes high radiosensitivity in cells that are irradiated just before or during mitosis. Apoptosis is a programmed cell death that can be caused by ionizing radiation. However, apoptosis is highly cell-type dependent, and in malignant cells, mitotic cell death is at least as essential as apoptosis [6, 9].

1.1.2. Cell cycle and radiosensitivity

All mammalian cells are proliferating by the mitosis cycle (figure 2). The cell cycle could be divided into four phases: mitosis (M), followed by G_1, DNA synthesis phase (S), G_2 phase, and mitosis again. The radiosensitivity of a cell is dependent on the phase of the cell cycle. The most sensitive are cells in the M and G_2 phases, and the most radioresistant are cells in the late S phase. The increased resistance in the S phase is due to homologous recombination repair between the sister chromatids, and it’s more likely to occur than if DNA is just replicated [6].

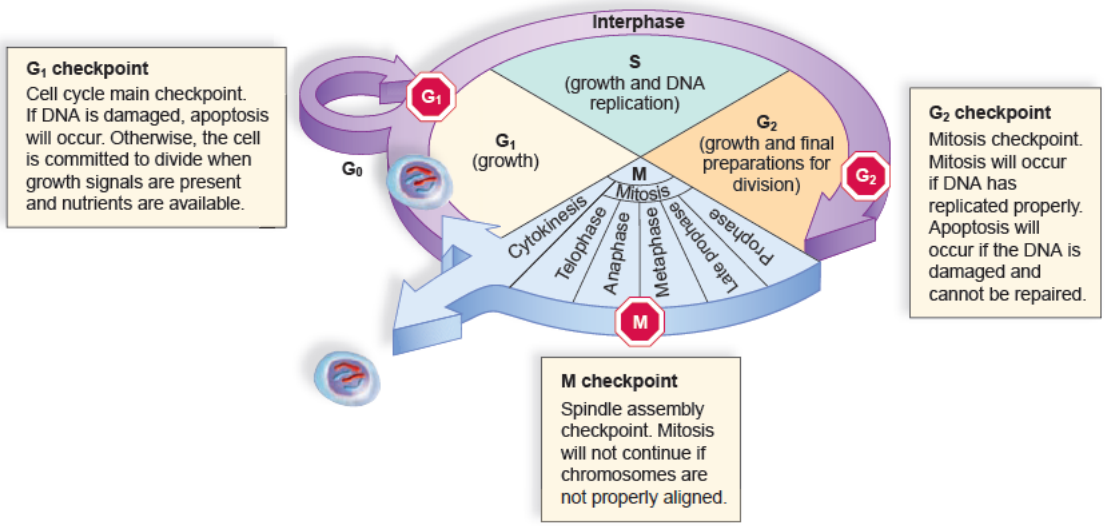

Fig. 2 Indirect and direct actions of ionizing radiation at the molecular level [7].

1.2. Main factors that describe the effect of radiotherapy on cells

1.2.1. Cell survival curves

In the early days of radiotherapy, the biological tissue response to the treatment was not fully known and was challenging to determine. Mathematical modeling of the dose-related response of the tissue helps to predict the possible reaction of biological tissue, understand it, and optimize treatment delivery [9, 10].

Mathematical models are based on experimental data. One of the critical points in experiments is the clonogenic survival (the survivor can retain its function and proliferate to produce a large clone or colony) of the cells [11]. Based on experimental data, mathematical models are constructed that reveal a link between energy deposition in cells and the probability of cell survival [11].

Probability of cell survival does not always mean cell death; this definition is much wider. For cells that are differentiated (are adjusted to maintain specific functions, e.g., nerve cells are adjusted to pass nerve signals; these cells also are not proliferating), death could be described as a loss of specific function. For cells that are not differentiated but are proliferating, the death would be a loss of reproductive integrity (reproductive death); this means that the cell or its progeny is unable to proliferate [6].

The most commonly used and simplest cell survival prediction model is the linear-quadratic (LQ) model. This model has become so popular due to its accurate fit for both clinical and experimental data. As mentioned above, the simplicity of the model also lets use it in the daily practice of radiotherapy: calculating compensation for missed treatment days, comparing different treatment schemes, and designing treatment schedules in clinical trials [10].

The basic LQ model represents the survival fraction (*SF*) of clonogenic or stem cells as a function of radiation dose (*D*). The general expression of this model is in the formula 1 below.

$$SF(D) = e^{-\alpha D - \beta D^2} \quad (1)$$

where D is a radiation dose; α and β – radiation sensitivity parameters.

The LQ model has two main parameters (sometimes called radiation sensitivity parameters): α and β. These parameters represent the sensitivity of cells to radiation; e.g., cells with higher values of these parameters are more sensitive to radiation than cells with smaller values. The ratio of α and β describes sensitivity to fractionation: A high ratio value indicates that cells are less vulnerable to the sparing effect of fractionation. The ratio value is usually measured in vitro by using a malignant cell line, but this value does not always correspond to the clinical radiobiological calculations. For better accuracy in a clinical environment, the α/β value could be calculated from the clinical radiotherapy data [10]. The radiation sensitivity parameter α is associated with cells that were killed by a single hit (low absorbed doses) and β is associated with multi-hit killing (high absorbed doses), and the ratio of this to parameters represents the dose, at which these effects (single hit and multi-hit) are equal [9].

At this time, the LQ model is still the most popular in clinical practice, but a number of studies prove that this model cannot be used for high-dose radiotherapy. Alternative models are crucial for higher accuracy in treatment planning, and it is highly recommended to create connections between LQ and other models, which could provide more accurate data about malignant and healthy tissue responses to ionizing radiation [12].

1.2.2. Linear energy transfer (LET)

Linear energy transfer describes the deposit of energy per unit path length when radiation or particles pass it [13]. In 1962, the International Commission on Radiological Units defined this quantity as follows: "The linear energy transfer (L) of charged particles in a medium is the quotient of dE/dl, where dE is the average energy locally imparted to the medium by a charged particle of specified energy in traversing a distance of dl" [6]. The unit of LET is (keV/μm) [6].

$$L = dE/dl \tag{2}$$

where dE is the average energy locally imparted to the medium; dL – distance.

Because LET is an average quantity, sometimes it could be misleading, but it provides a simple way, how to indicate the quantity of different types of radiation. Radiation could be divided into two groups: low and high LET emissions.

Table 1. LET values for different types of radiation [9]

Type of radiation	**LET value, keV/μm**
Photons or electrons	0,2
Protons	from 2 to 20
Heavier charged particles	100 and more

LET value is an important parameter to predict the possible damage to the critical target (DNA) in the cell. The high value of LET means, that ionization energy deposition will be distributed denser in DNA and greater damage will be made [9].

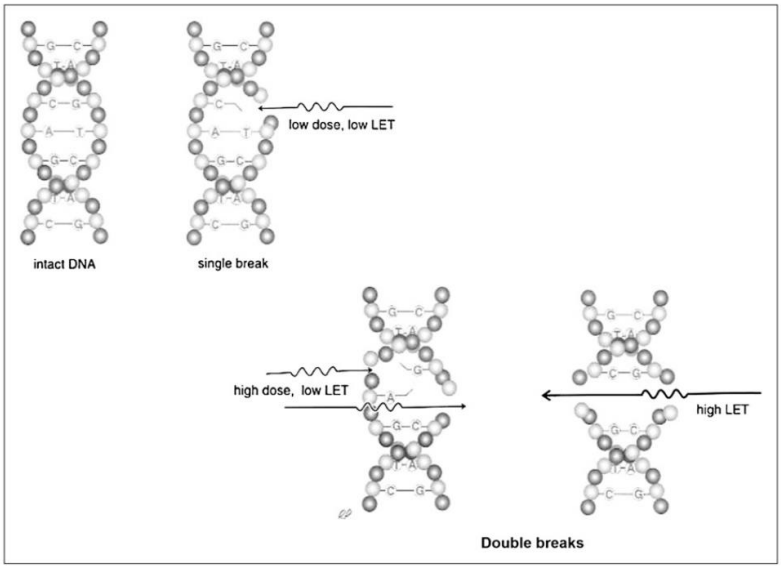

Fig. 3 Schematic comparison of high LET and low LET irradiation-induced DSB damage for DNA [14].

Figure 3 shows that radiation with a high LET produces double-strand breaks at DNA, but for low LET, higher doses are required to cause the same damage as radiation with a high LET [14]. Low LET with low doses tend to produce single-strand breaks, and these breaks are much easier and faster reparable. Radiation with a high LET has a tendency to produce more than one DSB with additional nearby strand or base damages. Later on, these small damages could overlap closely enough and produce additional DSB [9].

1.2.3. Oxygen enhancement ratio (OER)

In the early studies of radiotherapy from 1920, it was found that oxygen concentration is as important as the dose rate in the cell response to radiotherapy treatment [14]. The ratio of dosages provided in hypoxic to aerated circumstances required to accomplish the same biological effect is called the oxygen enhancement ratio (OER) [6]. The influence of oxygen concentration is most visible when irradiation is done by sparsely ionizing radiation (low LET values) and treatment is applied by densely ionizing radiation (high LET value), so the oxygen concentration is not important anymore. The correlation between the importance of the OER and LET is indicated in figure 4 below.

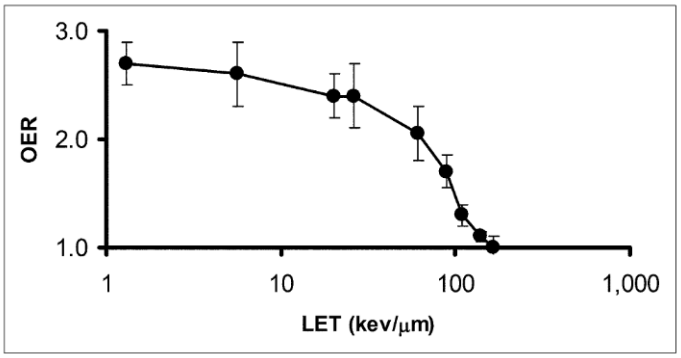

Fig. 4 The relationship between OER and LET [14].

Some studies suggest that radioresistance infected by hypoxia is due to the phenotype of the cell via signaling pathways, but the traditional explanation is that a higher oxygen ratio helps to produce more DNA in the case of indirect action [14]. The DNA reacts with free radicals (R•) and the break appears,

the DNA radical could be quickly „fixed“ by the reaction with the SH group. When the oxygen concentration is high, DNA radicals form connections with oxygen and create organic peroxide, which leads to the non-restorable form of the target (the chemical composition of DNA changes due to this reaction). Due to this reaction, the organic molecule (DNA) cannot repair itself and recover functional ability. In this case, the temporary SBS becomes permanent. This phenomenon is known as the oxygen fixation hypothesis [6].

1.2.4. Relative biological effectiveness (RBE)

Relative biological efficacy describes the quality of various types of irradiation. This concept was created for the comparison of different types of radiation. Absorbed dose is a quantity of absorbed energy per unit mass of tissue, although different types of radiation (when the dose of irradiation is equal) might elicit various biological reactions [6]. The RBE value is derived by dividing the absorbed dose of reference radiation (typically x-rays) required to generate a biological effect *x* by the absorbed dose of the test irradiation, $D_t(x)$, required to cause the same biological effect (formula 3) [14].

$$RBE(x) = \frac{D_r(x)}{D_t(x)} \tag{3}$$

where D_r is absorbed dose from reference radiation; D_t – absorbed dose from tested radiation.

The RBE value depends on: physical parameters, that describe radiation and delivery, and biological parameters of the biological system that was irradiated [11]. Due to various factors, it is hard to estimate the precise value of RBE, and it is usually done experimentally [11, 14].

Physical factors which are important in RBE evaluation:

- Absorbed dose.
- Dose rate.
- Quality of radiation (described by the spatial distribution of the energy imparted by the density of ionization per unit path length).
- The initial emission energy of the particle[9, 14]

Other factors:

- Biological background: different biological systems will provide different results. Even the same biological system cultured in different laboratories can react differently[11].
- The methodology used to calculate the absorbed dose for the reference and the test radiation. This factor could be reduced by using the correct methodology, which evaluates the true absorbed dose value or specific energy distribution [14].

RBE value for alpha particles varies from 3.5 (than the effect is cell killing) up to 10 (than the effect is cell phenotype changes) [7].

1.3. Alpha particles: effect on the cell, possibilities of use in therapy

In recent years, there has been a high focus on looking forward to improvements or alternatives in radiotherapy that would allow for more precise treatment with smaller healthy tissue toxicity. Alpha therapy has always been a field for deeper studies since its first application for patients with leukemia in 1995 [2]. Alpha particles with a high LET value and a short path length appear to be appropriate for widespread illness, tiny neoplasms, micrometastases, and individual tumor cells [2]. Alpha

particles are atoms of $^{4}He^{+2}$ with much bigger mass than electrons; they are monoenergetic, and the initial kinetic energy varies from 5 to 9 MeV. Alpha particles hold close to a linear path, and destruction can occur all along the path. All these characteristics lead to highly effective damage for the cell; a single alpha particle can produce DSB, which will lead to cell death. It has 500 times higher cytotoxicity than beta particles. One other important characteristic of alpha particles is their short particle range. This parameter suggests alpha particles as a great option for treatment delivery to metastases and minimizes toxicity for healthy cells around them [2].

1.3.1. Alpha particles for therapy

Alpha particles could be introduced in radiotherapy in two different ways: by the use of a particle accelerator (hadron therapy) and by the use of radiopharmaceutical therapy (RPT). In hadron therapy, particles gain benefits from energy deposition in the path in comparison with photons. The maximum photon energy deposition occurs near the tissue's entrance and declines exponentially with depth. In contrast, the maximal energy deposition of light or heavy ions occurs within the Bragg peak, at a depth dictated by the particle's energy, and the minimal energy deposition occurs before the peak [15, 16]. Figure 5 shows depth-dose profiles for γ-rays and ^{12}C ions: the maximum energy deposition of γ-rays is very close to the surface and widespread, while the maximum energy deposition of ^{12}C ions occurs more neatly.

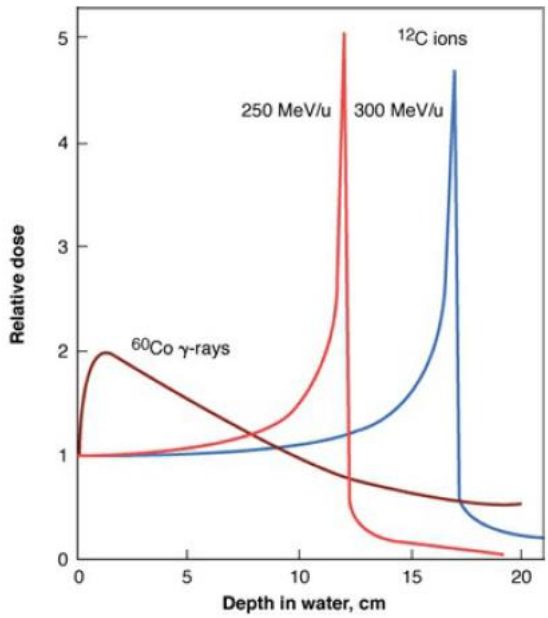

Fig. 5 Depth-dose profile for γ-rays and ^{12}C ions [6]

Radiopharmaceutical therapy (αRPT could sometimes also be called targeted alpha particle therapy (TAT)) works in a different way than hadron therapy. The radiation is delivered not as a beam of protons or ions but as an emission from a radioactive element (a radionuclide) that is conjugated to chelating agents (for example, peptides, antibodies, or tiny compounds that recognize tumor-associated antigens or cell-surface receptors) which bind to tumor cells or elements of the tumor microenvironment [7]. The ability to deliver α-particles directly to tumor cells using tumor-targeting molecules is unique to RPT. Due to the comprehensive benefits of α-particles mentioned in the section above, αRPT gains an advantage against tumors that are resistant to other forms of cancer therapy.

It is known that there are subpopulations of cancer cells that are more resistant to radiation and require a higher dose of irradiation to be killed (due to the healthy tissue toxicity and precision of conventional radiotherapy, higher radiation doses are limited due to the radiosensitivity of healthy tissue around the target). These cells are known as cancer stem cells. They are tumorigenic and can self-renew and differentiate into any type of malignant cell. Eliminating cancer stem cells is critical for preventing recurrence. αRPT is an option to target groups of cells and provide successful treatment under this condition [18].

1.3.2. Applications of targeted alpha therapy in clinical practice

Prostate cancer (PCa) is the most common cancer-related death among males. When the cancer is detected early (before spreading metastases), it is possible to cure the patient by removing the tumor via surgery, but if the cancer becomes metastatic, the possible option is androgen deprivation therapy, which could hold PCa in control for 18 to 24 months. After this period, the PCa becomes castration-resistant. It is clear that conventional therapies just treat the bulk of the tumors without preventing relapses in the future, and alpha particle treatment could be a possible option to prevent relapses of PCa [18].

^{223}Ra dichloride, also known as Xofigo®, is the first approved α-particle emitting specimen that is used for castration-resistant prostate cancer with symptomatic bone metastases. ^{223}Ra is a calcium mimetic that preferentially binds to hydroxyapatite accumulation, such as bone metastases in PCa [19].

^{223}Ra has proved that the concept of TAT is an effective treatment strategy for PCa. In the II phase of the ALSYMPCA trial, it was found, that patients treated with ^{223}Ra survived 14.9 months, while the placebo group survived 11.3 months. The treated patients also showed a significant increase in health-related quality of life and a longer time period until the first symptomatic skeletal occurrence [19].

Xofigo® has been used for longer than 10 years in clinical practice, as an effective agent for safe treatment of PCa metastases in bones. However, there are more radionuclides showing promising PCa treatment results: ^{225}Ac, ^{213}Bi, and ^{227}Th. Many preclinical and clinical studies are investigating the therapeutic options and potential of TAT for PCa treatment [19, 20].

Prostate cancer is not the only metastatic cancer that could benefit from alpha therapy. This therapy could also be used for the treatment of early brain metastases (which develop frequently in patients with breast cancer), breast cancer, glioblastomas, and neuroendocrine tumors [21–24]. Patients with these malignancies usually have no option for treatment, especially because of the late diagnosis of the disease. An innovative, and precisely targeted therapy is one of the best options for treatment. For example, brain metastases could be treated using whole-brain radiotherapy or image-guided stereotactic radiosurgery, but both techniques are limited in their therapeutic effect and may also induce cognitive deterioration in the case of multiple metastases [21]. The possible choice in this case is TAT with an application of lead-212, copper-64, to lutetium-177 radionuclides.

1.3.3. Reasons why targeted alpha therapy is not widely used for cancer treatments

The properties of alpha particles (short range, high LET, and RBE values) look like a perfect combination for cancer treatment. Recent diagnostic methods are very effective in detecting cancer.

However, there are a lot of patients who experience remission later in their lives because not all malignant cells and metastases are removed [25]. The TAT could be included in the treatment procedure because it enables the removal of metastases whose diameter is too small to remove with other treatment techniques. This would help to save more lives and make significant savings in the healthcare budget [25].

Despite all the advantages listed above, the TAT is not a common procedure in the healthcare system. Since 1995, there have been numerous pre-clinical and clinical studies on the use of alpha particles in treatment, but there are several obstacles that prevent widespread application [10]. It is necessary to investigate new delivery strategies, enhanced chelation chemistry, pharmacokinetic and dosimetry modeling approaches, and alpha particle emitter production procedures. To determine the ideal radioisotopes, dosage regimens, and treatment approaches, more preclinical and clinical research is required [3, 4].

1.4. Cell cultures

1.4.1. Types of cell cultures: advantages and disadvantages

Cell culture as a research model was first implemented in 1907 in research about the origin and development of nerve fibers. After the first application, cell cultures started to be widely used in biological experiments. The technology improved, and cell banking was established for effortlessly conducted experiments. Cell cultures in cancer research are an unchangeable tool for a better understanding of tumor biology, response to treatments (chemotherapy and radiotherapy), and even the discovery of new options for treatments [26].

Cell culture refers to the removal of cells from tissue before their growth in a favorable artificial environment. Later on, cells grow in an artificial environment where proper conditions for consistent growth are ensured: a medium supply of essential nutrients (amino acids, vitamins, minerals, carbohydrates), growth factors and hormones, and O_2 and CO_2 gasses. The pH, osmotic pressure, and temperature are also regulated to ensure the most appropriate conditions for cells [27].

At the beginning research was conducted on 2D cell culture, in which a monolayer of cells grew on an adhesive surface. However, 3D environment conditions cannot be replicated in a 2D cell culture. It was found that 95% of the human subjects in the trials utilizing immortalized tumor cell lines cultivated in 2D culture methods failed to respond to medication. It suggested that the 2D cell culture model might not be a reliable model to research new drugs. According to the findings of the other study, drug resistance that was developed in mice's EMT6 tumors was entirely lost when the cancer cells were separated and cultivated in monolayers, but it could be fully recreated when the cells were cultured in a three-dimensional system [26, 28].

Even though 2D cell culture has several established drawbacks, it is still the preferred method since it is easy to use and yields preliminary findings. 3D cultures are a superior choice for improved *in vitro* research since they yield more accurate data. The capacity of 3D cell culture to generate relationships between cells and between cells and extracellular matrix is by far its greatest advantage. Cells are encouraged to form spheroids in 3D cell cultures. Particularly in cancer and stem cell research, the 3D spheroid culture is thought to be a better model for predicting *in vitro* cell-based tests and could have significant physiological significance for preclinical drug discovery [26]. The summarized comparison of 2D and 3D cell cultures is provided in the Fig. 6.

2D	3D
• Cell-cell contact is limited	• Cell-cell contact is dominating
• Cell-flat, plastic surface contact is dominating	
• Contact with ECM only on one surface	• Cells remain in contact with ECM
• No gradient	• Diffusion gradient of nutrients, waste, oxygen and drugs
• Co-culture cannot create a microenvironment	• Co-culture can mimic microenvironment
• No resistance for anticancer drug	• Resistant to anticancer drugs (mimic tumor morphology)

Fig. 6 The comparison of 2D and 3D cell cultures [29]

The cells are grown in 3D cell structure; the cell-cell and cell-matrix interactions are not perfectly mimicked but are close enough to induce morphological alteration of cells to not be relatively flat but closely resembling their natural shape in the body. Further, the spheroid structure unsure conditions to establish various stages of cells: proliferating, quiescent, apoptotic, hypoxic, and necrotic cells due to the gradients of nutrients and oxygen levels [26]. Fig. 7 schematically represents different cell cultures (monolayer and spheroid) and how the various stages of cells are established in the 3D cell structure. Due to the high amount of nutrients, the proliferating cells are mainly in the outer layer of the spheroid. This cell directly contacts the culture medium and directly absorbs nutrients. Due to a lack of nutrients, growth factors, and oxygen in the center of spheroid cells, they are mainly in hypoxic or quiescent stages. 3D cell culture was shown to be more suitable for longer experiments; they can last up to 3 weeks, while the monolayer (2D cell culture) can be cultivated for less than a week. Later on, 100% of cell confluence is reached, and results cannot be trusted any longer. Due to this reason, 3D cell culture is the first option for determining the long-term effects of the treatments [26].

From a critical perspective, it is important to remember that 3D cell systems' complexity is both a benefit and a drawback. There will always be a number of issues that can only be addressed by research employing single cells or systems devoid of cells. At the same time, studying biological systems for their applicability in vivo cannot be entirely replaced by 3D cells [28].

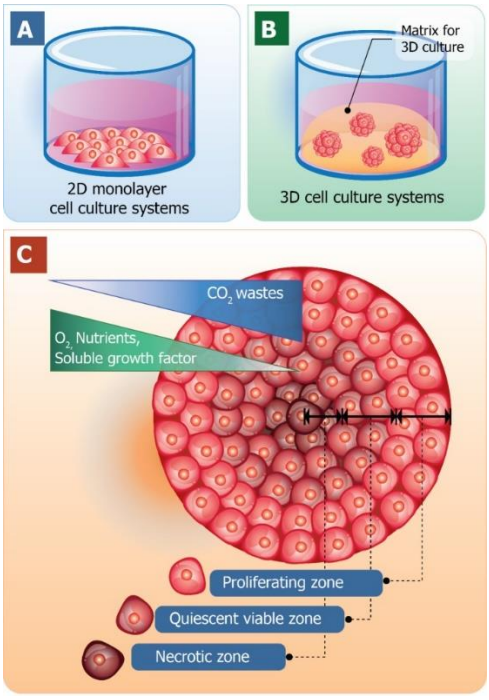

Fig. 7 A: The 2D cell culture (monolayer); B: the 3D cell culture (spheroid); C: the different areas of the spheroid where various stages of cells are established [26].

1.4.2. Cell cultures as a model for radiobiological experiments

In radiobiology, cell culture studies are crucial. It's used to simulate how ionizing radiation interacts with tissue; a lot of radiobiology dogmas are derived from the molecular and cellular reactions of cells cultured in a monolayer (2D cell culture) [5]. The "clonogenic assay," which assesses the cell's reproductivity, stands in for both the sensitivity of the tissue and the "gold standard" of the radiation treatment plan. While these methods are widely acknowledged for their valuable contributions to the understanding of the mechanics behind biological reactions to radiation, 2D systems give an unrealistically simplified picture of reality [5]. Over the years, the difference between expected and obtained results after radiotherapy treatment has become increasingly evident and could be related to higher sensitivity to radiotherapy than cells grown in monolayer. Nevertheless, there is currently an absence of research on the use of 3D models in radiation response investigations. It might also be the cause of promising preclinical medication candidates' clinical trial failures, which expose their limited efficacy [5].

In the past, radiobiological models have been used to predict the radiobiological response; experimental and clinical data have best verified the linear-quadratic model. Although the importance of the LQ model in clinical practice has been demonstrated, concerns about its applicability still exist because all of the data came from experiments using two-dimensional cell cultures, and there is proof that both additional variables, like the tumor microenvironment, and genetic factors can influence the tissue's response to ionizing radiation [5]. Using LQ models derived from 2D cell cultures in radiotherapy treatments may result in an inaccurate prediction of the risk-benefit ratio and an underestimate of the radiation dose required to eliminate the tumor [5].

Two major types of malignant cells compose a tumor: differentiated cells and small quantities of cancer stem cells. It has been established that cancer stem cells play a major role in tumor growth, maintenance, metastasis, and resistance to chemotherapy and radiation. Because stem cells can survive and multiply after therapy, even the treatments themselves may increase the stem cell population [5]. Research findings indicate that the resistance of cancer stem cells to therapy derives from their rapid and efficient DNA repair processes, as well as their capacity to rearrange the tumor microenvironment. Recent research has shown that cancer cells' stem characteristics are strongly influenced by the environment in which they are developing. Suzuka et al. [30] have shown that when seeded in a 3D structure made from a double-PEG hydrogel network, any of six human cancer lines or brain cancer cells removed from glioblastoma patients quickly trained themselves into cancer stem cells. That study is just one of many that demonstrate that stemness gene expression is upregulated in a 3D environment, regardless of the type of 3D structure.

Tumor cell physiology and radiation response are strongly influenced by their surroundings. Typically, the surrounding environment cannot be replicated or provided in two-dimensional cell cultures. Specifically, 2D cell cultures growing on a flat surface, are non-dimensional and cannot sustain a 3D environment. Furthermore, the tumor microenvironment lacks sophisticated 3D architecture, and 2D cell cultures have a low potential to differentiate. Consequently, the intracellular interactions at the foundation of tumor growth, dissemination, and response to chemotherapy and radiation therapy cannot be replicated by these models [5]. Fig. 8 schematically represents differences between 2D and 3D cell cultures.

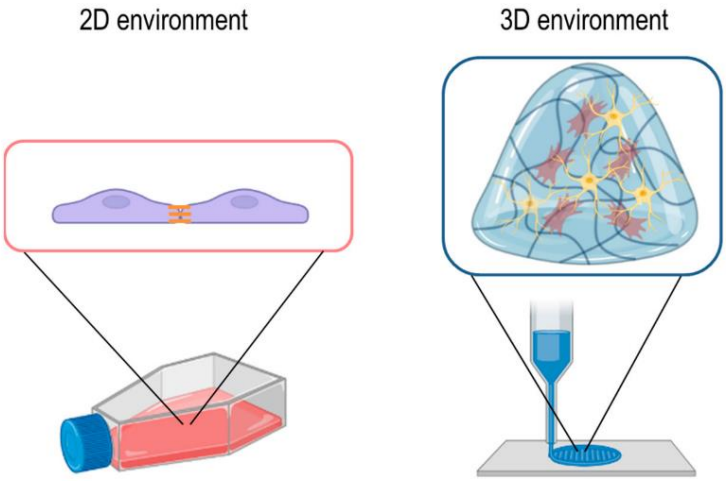

Fig. 8 schematic representation of 2D and 3D cell cultures [5]

1.5. 3D cell culture in radiopharmaceutical cancer research

3D cell culture is playing a bigger role in preclinical cancer research. They offer information before to the start of investigations using animal models and can sometimes be used in place of or in addition to animal experiments. As the 3D system grows, it reflects physiological phenomena like oxygen and nutrition gradients and exhibits a greater degree of structural complexity and diversity in cell interactions. To gain a better knowledge of solid tumor growth, therapeutic response, and resistance mechanisms, these features are irreplaceable. 3D models can be divided into three groups: organoids, scaffold-free models, and scaffold-or matrix-based models. Occasionally, a collection of cells that form loose packages but do not form compact structures may be referred to in the literature as multicellular tumor spheroids; in this instance, the group of cells is incorrectly labeled as a spheroid [31].

It has been demonstrated [31] that spheroids resemble their parent tumor considerably more. The explanations they provide are predicated on average correlation coefficients calculated from the genetic profiles of parental tumors and 2D and 3D cell cultures. Spheroids were shown to have a higher correlation coefficient (about 0.89) than monolayer culture, which had a correlation coefficient of only 0.62. Furthermore, even after a brief period of incubation, half of the examined 2D cultures displayed significant genetic alterations, in contrast to the more genetically stable spheroid cultures [32].

Owing to all these benefits, 3D models are being used more and more in radiopharmaceutical research to examine responses. The primary goal is to characterize new radiotracers for their in vitro use in nuclear medicine imaging with either single-photon emission computed tomography or positron emission tomography. The synthesis of radiolabeled compounds with appropriate radionuclides—typically employed for alpha and beta emitters—also heavily depends on these models. Radiosensitizers and radioprotectants could be tested as therapeutic methods using the 3D cell structure. Here, a carefully planned study could support the three R's of animal research: replacement, reduction, and refining [31].

Over 90% of cells in monolayer cultures proliferate, whereas the proportion of proliferating cells in spheroids varies with spheroids' size; larger spheroids proliferate less. Size-dependently, the fraction

of cycling cells drops from 70% to 40%. It was demonstrated that slow-growing spheroids are more resilient to the therapeutic effects of radiation because they include fewer cells in the radiosensitive G_2-M phase [31].

Spheroids can be re-incubated in media to allow for possible growth to study the impact of possible radiotherapeutics or other substances on cell viability. The therapeutic agent may be given multiple times to replicate radiation in a clinical setting [31].

The team of scientists Raitanen et al. looked forward to two of the most common cell lines reactions to the irradiation of x-ray photons (1, 2, 4, 6, 8, or 20 Gy) with the parameters 200 kV and 20 mA and a focus size of 5,5 m with a 0,5 mm copper filter and a 3 mm aluminum filter. They compared the reactions of 2D and 3D cell cultures. Three distinct cell lines—PC-3, LNCaP, and T-47D—were employed in the investigation, and many characteristics were examined, including viability, growth behavior, and the quantity of DSB. The study's findings support the significant distinction in how 2D and 3D cultures react to radiation. In every cell line, the spheroids exhibited higher radioresistance in comparison to the corresponding monolayers [33].

1.6. 3D cell cultures in studies of targeted radionuclide therapy

3D cell cultures have gained popularity among targeted radionuclide therapy studies. 3D cell cultures are used to analyze the effects of different chemicals and the possible effects of different types of radionuclides. These studies are innovative, but quite rare at the moment.

Studies in targeted radionuclide therapy could be separated into two groups according to the type of radioactive decay: alpha or beta. In this work studies related to alpha emitters are of great interest, but relevant studies exploring beta decay are also useful in terms of investigation methodology and obtained results.

^{177}Lu was identified as a source of beta particles and ^{225}Ac, ^{111}In, ^{223}Ra, ^{224}Ra, and ^{212}Pb as sources of alpha particles [33–37]. in several studies. All these studies used 3D cell culture, but the cell lines were different. The authors provided the results on how the treatment affected the size of the spheroid.

Seifert et al. analyzed the radioprotective effects of pseudohypoxia against external irradiation and beta particles emitting ^{177}Lu. The main point of this study was to analyze how hypoxia-inducible factor 2 alpha (HIF2α) was associated with increased radioresistance to external irradiation. Scientists used mouse pheochromocytoma cells to form spheroids using a liquid overlay technique. The spheroids were irradiated by external X-rays by single-dose exposure between 4 and 40 Gy (irradiation occurred from 6 to 9 days after cultivation started). The irradiation-induced shrinkage, followed by regrowth or disintegration, whereas the control group grew continuously up to diameters of 873±14 μm. Over a 35-day follow-up period, the regrowth of treated spheroids revealed three distinct dose-effect scenarios: 1) the regrowth of all spheroids with a dose-dependent delay (irradiation dose: 4 to 16 Gy); 2) the partial regrowth of spheroids with increasing fractions of disintegrated spheroids (irradiation dose: 20 to 25 Gy); and 3) the sustained control of all spheroids per group (40 Gy). One possible treatment option, as single-dose external X-ray irradiation is not frequently used, was to incubate spheroids in [^{177}Lu] $LuCl_3$ for six days. This was thought to be a more basic kind of radionuclide therapy. The range of the activity concentration was 0 to 1,25 MBq/mL, roughly corresponding to the range of irradiation dosages from 0 to 10 Gy. Spheroids also supplied the three response models following this treatment, similar to that of external irradiation.

The spheroids had negative growth rates and dose-dependent shrinking when they were treated with 0.75 MBq/mL to 1.25 MBq/mL. Following the final analysis, scientists concluded that lower absorbed doses of [^{177}Lu]$LuCl_3$ were needed to produce outcomes comparable to those of external irradiation [36].

Raitanen et al. [33] analyzed the possibility of using ^{177}Ac in targeted radionuclide therapy and compared the results for the 2D and 3D cell cultures. In this study, two cell lines were used: PC-3 and LNCaP. Spheroids were treated with activities ranging from 0 to 3.2 MBq. PC-3 spheroids didn't show significant differences in size up to 3.2 MBq, while LNCaP spheroids started to show differences at the lowest applied activity (0.01 MBq). Treatment with 0.05 MBq had a high efficiency, but it was not significantly different from 0.2 or 0.4 MBq treatments. Spheroid diameters were monitored 0, 7, 14, and 20 days after the treatment, and the difference in spheroid shape and growth rate is highly dependent on the cell line. Scientists discovered that 2D cell culture showed higher viability. After the Monte Carlo simulation, it was found that 3D cell culture receives a higher dosage from the same treatment activity. This explains the lower viability of 3D culture versus 2D culture. One explanation for the gradual rise in spheroids' sensitivity to radionuclide therapy could be that the compound is retained in the three-dimensional structure, resulting in a longer treatment duration and an increased bystander effect. Nevertheless, further research is necessary to determine whether the magnitude of this impact is comparable to that of in vivo malignancies [33].

The same cell line, PC-3, as in a Raitanen et al. study [33], was used in an Abramenkovs et al. [37] study to analyze the effect of ^{223}Ra. In this study, results were compared from 2D and 3D cell cultures. Additionally, 22RV1 and DU145 cell lines were also used. Spheroids were produced from 1000 and 500 cells on the low-attachment cell plates. Spheroids were treated with a ^{223}Ra solution, whose specific activity varied from 0 to 500 Bq/mL. The survival of all three cell lines significantly decreased after increasing the specific activity concentration of ^{223}Ra. The spheroid size was assessed at 0, 5, and 10 days post-treatment; the size changes were obviously dependent on treatment specific activity concentration. Even though alpha particles from ^{223}Ra decay have a maximum range of 70 μm in tissue, exposure to ^{223}Ra distributed in the growth media was able to impair cell survival in monolayers and 3D spheroids and produce substantial levels of apoptosis [33].

Jalloul et al. [38] analyzed the possibility of using ^{225}Ac as a potential radionuclide for theranostic purposes. During the decay, ^{225}Ac emits alpha particles and gamma rays, which makes it suitable for diagnostic (single photon emission computed tomography) and therapeutic purposes. ^{225}Ac is gaining popularity in studies, but due to restricted global accessibility, it is hard to make extensive clinical studies [36]. Zhu et al. analyzed how ^{225}Ac could be used for solid tumors (the diameter of the spheroid is bigger than 400 μm). The diffusing properties of ^{225}Ac were improved by encapsulating 225Ac into liposomes. Three cell lines were used to form spheroids and analyze treatment efficiency: BT474, MDA-MB-231, and MCF-7. Different-size spheroids were produced by using 400 (BT474), 250 (MDA-MB-231), or 125 (MCF-7) cells for formation. After one week of formation, spheroids were incubated for 6 hours in the solution with ^{225}Ac-labeled carriers (18.5 kBq/mL), and after treatment, the spheroids volume was monitored till the control group stopped growing. This work developed an alpha particle emitter-based diffusion-assisted solid tumor therapy method. This approach, which adheres to general nanoparticle-based delivery rules for tumor uptake, relies on fast-diffusing radioactive species released within the tumor interstitium from nontargeted liposomes to improve the intratumoral alpha particle emitter distribution for more uniform tumor irradiation [35].

A more interesting study was published by Juzeniene et al. Scientists analyzed the dual targeting with $^{224}Ra/^{212}Pb$ conjugates application for targeted alpha therapy. This approach suggests a dual targeting solution, which could be a promising approach for the treatment of metastatic cancers with bone and soft tissue lesions as well as skeletal metastases of mixed lytic/osteoblastic nature. The effect was associated with LNCaP cell line spheroids (prostate cancer). The specific activity of the treatment was 1 kBq/mL, and the volume of spheroids was monitored at 0, 7, 14, 21, 28, and 35 days post-treatment. Spheroids were formed by liquid overlay techniques from a suspension of 500 cells per 100 µL. The dual targeting solutions that utilize both the cell-directed complexes of ^{212}Pb and the bone-seeking ^{224}Ra appear to be a potential way to treat metastatic malignancies that present with soft tissue and bone lesions, as well as skeletal metastases of mixed lytic and osteogenic character [34].

2. Methods

2.1. Cell cultivation

2.1.1. The culture media

One of the most crucial elements in cell culture is the culture media. Rich in nutrients, growth stimulants, and hormones, the culture medium also controls the culture's pH and osmotic pressure. The most widely used standard media for the cultivation of many broad-range mammalian cell types are the media from Roswell Park Memorial Institute (RPMI 1640) and Dulbecco's modified Eagle medium (DMEM). These media often include pH buffer systems, vitamins, amino acids, carbs, and salts. Growth factors, lipids, proteins, and hormones are usually absent from basal medium, hence serum supplementation is essential [39, 40].

The most crucial component for cell adhesion and proliferation is serum. As an enrichment medium, it gives the cells nutrients, lipids, and hormones. It can facilitate the transport of lipids and enzymes and control the permeability of cell membranes. Although there are different animal serums available, fetal bovine serum (FBS) is the most widely used. Depending on the type of cell, different amounts of FBS are added to the media; nonetheless, a typical concentration ranges from 5 to 20% (v/v) [39, 40].

Protection from biological contamination (bacteria, yeast, and fungi) could be achieved by adding antibiotics and anti-myotics to cell culture media (typically penicillin and streptomycin). It is a recommendation to avoid the permanent use of antibiotics and try to implement strict aseptic working practices [39, 40]. To ensure these conditions, any maneuver with cells is made in a laminar flow cabinet (Fig. 9).

In the research project, RPMI 1640 (*biowest*) media with L-Glutamine was used for the cell cultures. It consists of 89% RPMI 1640 media, 10% FBS, and 1% antibiotics.

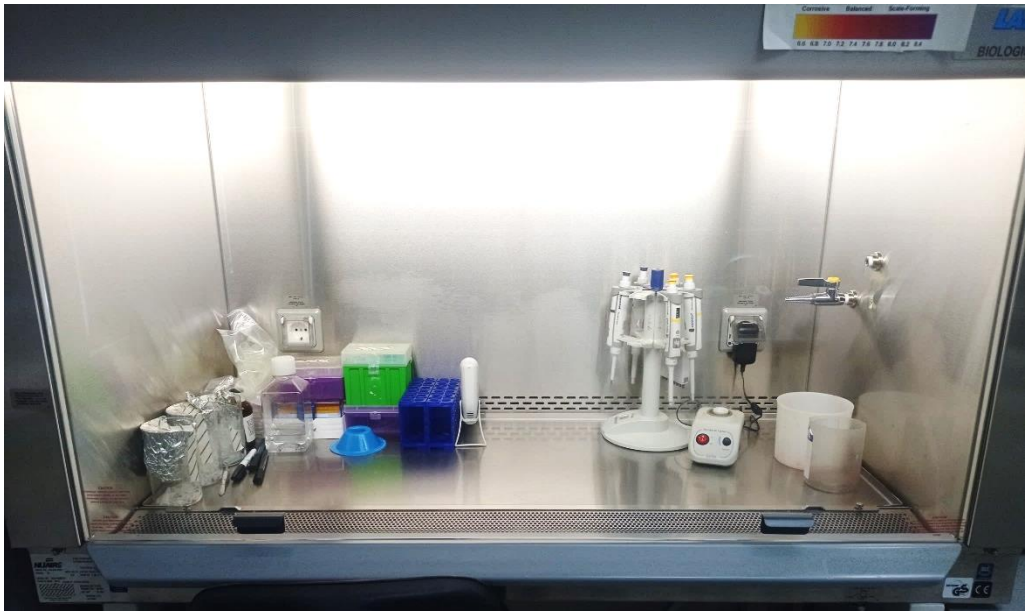

Fig. 9 A laminar flow cabinet at the National Cancer Institute, biomedical physics laboratory

2.1.2. Maintenance of cell culture

Cell culture growth could be divided into four phases [41]:

- Lag phase: the beginning of cell culture. Cells need time to adapt to the new environment. Due to this phase, cells are not dividing.
- Log phase: at this phase, cells are actively dividing, and this phase is the best for the experiments.
- Stationary phase: when cells overfill the environment, the dividing process starts slowing down. If the cell culture is not reseeded at this phase, the culture is going to be in cellular stress, which will lead to the death phase.
- Death phase: the culture is under cellular stress and cells are not dividing anymore. The properties of the cell culture can also be changed, and the results from experiments cannot be trusted anymore.

The cell culture subculturing or passaging ensures that cells are in the log phase and the metric cell density in the monolayer is confluence. Adherent cultures should be passed before they reach 100% confluency.

Cell lines in culture vessels before passaging

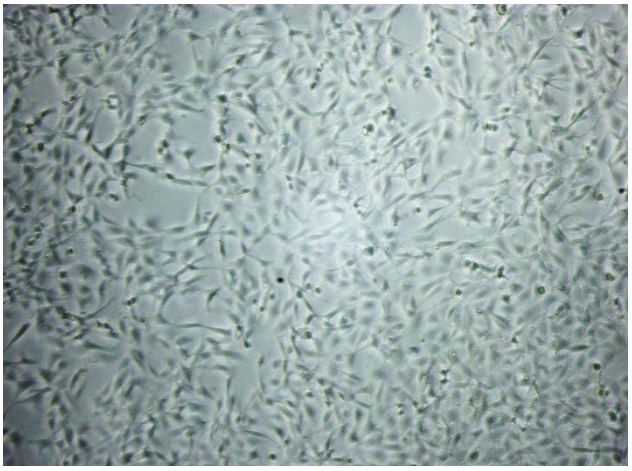

a)

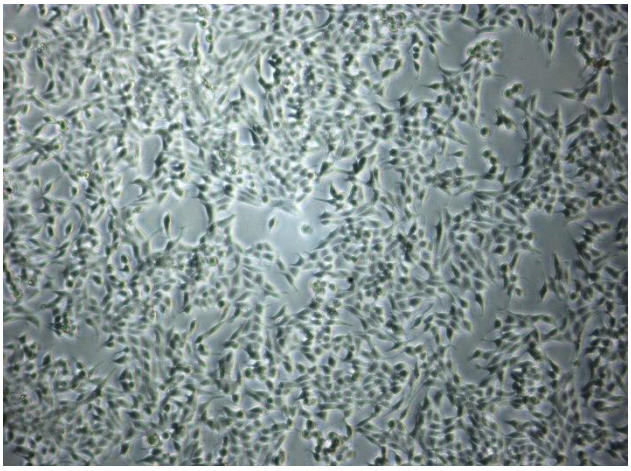

b)

Cell lines in culture vessels after passaging

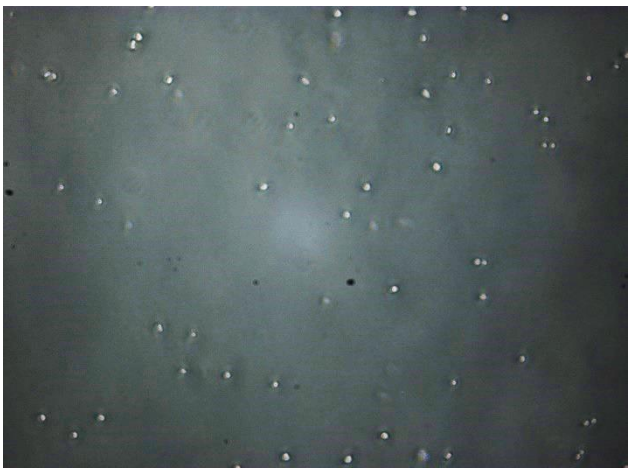

c)

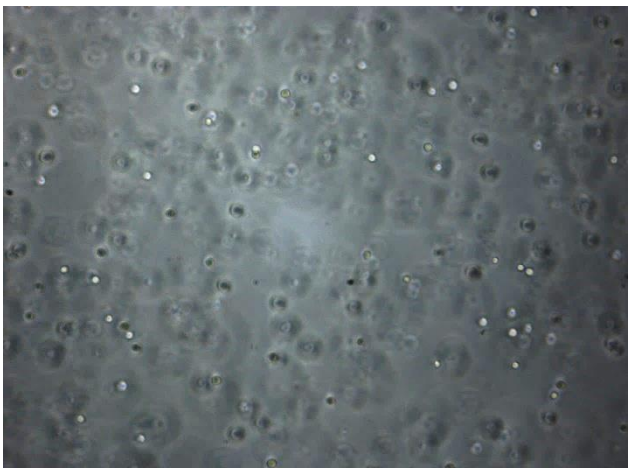

d)

Fig. 10 Glioblastoma (a, c) and prostate cancer (b, d) cell before and after passaging

Steps of passaging [40]:

- The medium from the culture vessel should be removed, and cells should be washed with a balanced salt solution (DPBS, *Corning*).
- To detach adherent cells from the surface of the culture vessels, enzymatic dissociation could be done by the solution of the enzyme trypsin (0.05% trypsin solution). The culture vessel should be incubated with the trypsin solution for about 2 minutes.
- Then around 90% of cells are detached, the trypsin and cell mixture is dispersed with medium, and cells are transferred to a conical tube for centrifugation (centrifugation parameters: 200g for 5–10 minutes).

Fig. 11 Centrifuge used in this research project for the collection of cells

- After centrifugation, the cell pallet (marked by red dashes in Fig. 12) should be suspended in a small amount of fresh medium, and a small amount of cell suspension should be removed for cell counting.

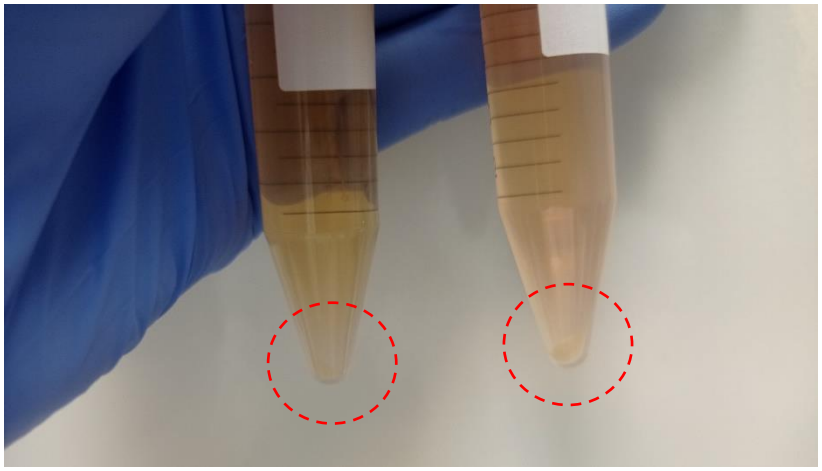

Fig. 12 Cell pallets after centrifugation

– Cell counting provides the required information for the total number of cells for the new cell culture formation in the new cell culture vessel. Cell counting by using a Malassez hemocytometer. The total number of cells in 1 ml is equal to the mean value of the number of cells in at least five squares marked by red circles in Fig. 13 multiplied by 10^{-5}.

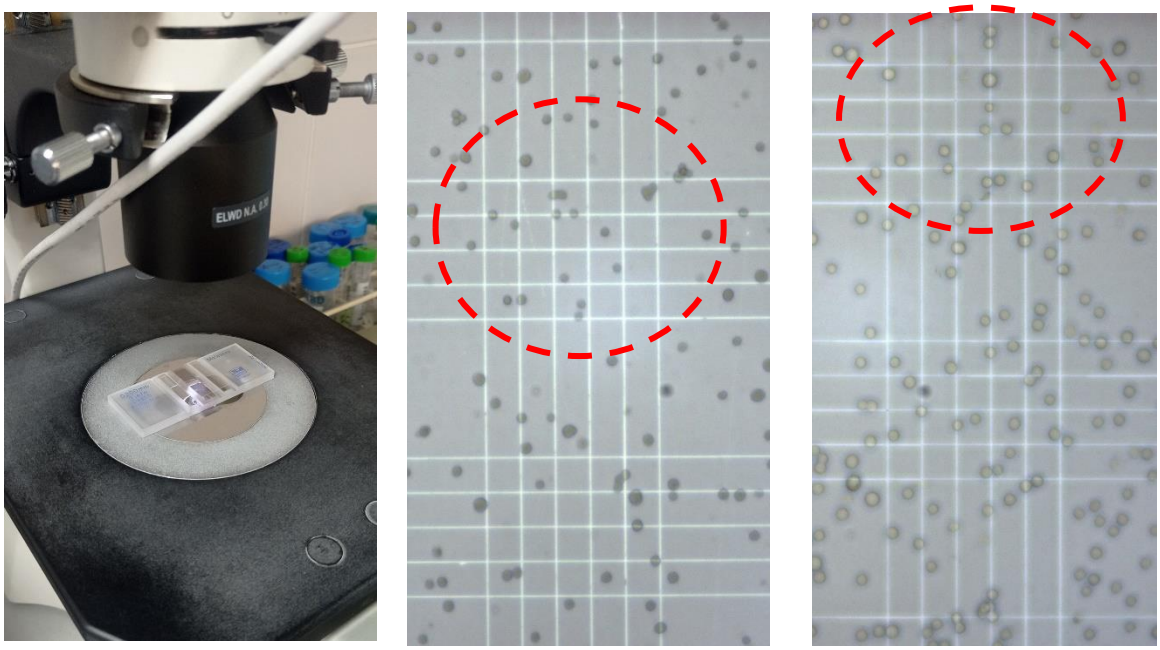

a) b) c)

Fig. 13 Cell counting: the hemocytometer is placed on microscope table (a), and the view observed from the microscope (magnification is equal to 10 times): glioblastoma (b) and prostate cancer (c) cell lines

– When the required number of cells are transferred to the new cell culture vessels (1,000,000 prostate cancer cells and 300,000 glioblastoma cells), cells are returned to the incubator (Fig. 14).

Fig. 14 Incubator “Binder“

2.2. 3D cell culture – spheroids formation

Cell aggregates known as spheroids self-assemble in conditions that prevent them from adhering to a flat surface. Extracellular matrix proteins and membrane proteins (integrins) enable the formation of spheroids [29]. The ways that could be used for formation could be divided into three groups:

- Suspension cultures on non-adherent plates;
- Cultures in concentrated medium or gel-like substances;
- Cultures on a scaffold.

Spheroids, according to their shape, can also be separated into three groups:

- Tight spheroids;
- Compact aggregates;
- Loose aggregates.

Different 3D cell culture methods have their advantages and disadvantages; a precise comparison of methods is shown in Fig.15 below.

Type of 3D system	Description of cell culture	Advantages	Disadvantages
Suspension cultures on non-adherent plates	• Single cells are seeded on non-adherent plates with medium • 3D structures can be observed after 3 days of culture	• Simplicity, easiness and speed of conducting culture • Bacterial plates or non-adherent culture plates can be used but only for some cell lines • Cells can be easily extracted from the medium and used for further experiments	• Some cell lines need expensive plates coated with specific materials, for example polystyrene or covalently bound hydrogel, because of strong adhesion abilities of cells • Formation of aggregates of cells as a result of cells' movement in medium
Cultures in concentrated medium or in gel-like substances	• Single cells grow in medium containing substances with gelling properties: i) dissolved low-melting agarose with cell medium is poured on plate and incubated until solidifying to obtain the first, lower layer; the top layer consisting of agarose and the medium with single cells is added; ii) the cells are flooded in Matrigel (multiprotein hydrogel) • 3D structures can be observed after 7 days of culture	• Soft agar allows to study both the growth of a single cell regardless of attachment and the phenomenon of escape from anoikis • Cells cultured in Matrigel can be easily recovered for further analysis • Cells in Matrigel have three-dimensional interactions with the local environment and form tissue-like structures • Used to study the aggressiveness of the cells and their potential for metastasis	• Difficulty in obtaining spheres for certain lines, inconvenient and time-consuming preparation of the two layers of agar and requirement of long-term cultures • Low repeatability of the results • The difficulty of extracting cells from the agar and immunofluorescence staining of spheres, • Materials constituting the Matrigel contain endogenous bioactive ingredients that influence the structure formation
Cultures on scaffold	• The cells can migrate among fibres and attach to the scaffold, made of biodegradable material such as silk, collagen, laminin, alginate, and fill the space among fibres, grow and divide	• System is compatible with commercially available functional tests, as well as with DNA/RNA and protein isolation kits • Easy to prepare for immunohistochemical analysis	• Cells attached to the scaffolds flatten and spread like the cells cultured under adherent conditions • Scale of scaffolds and topography of cell distribution may cause various behaviour of the cell • Materials used to construct the scaffold may affect the adhesion, growth and cell behaviour • Cell observation and cell extraction for some analyses are restricted

Fig. 15 Comparison of different 3D cell culture formation methods [42]

In the research project, 3D cell cultures were formed by the scaffold-free method. It could also be called the "forced-floating“ method because the approach uses low adhesion plates. Cell culture plates could be coated with 0.5% poly(2-hydroxyethyl methacrylate) or 1.5–3% agarose to prevent cell adhesion to the surface of the well. Due to this, cells start to make cell-cell interactions, and the spheroid is formed [31]. The main advantages of this method are easy maintenance, the possibility of controlling the size of spheroids (with diameter variations below 5%), the high number of spheroids per plate, and cost efficiency [29, 31, 43, 44]. This method allows cultivating spheroids for up to 3

weeks and making long-term experiments for long-term effect determination, such as tumor growth kinetics [26, 44].

In the experiment, spheroids were formed by the „forced-floating“ method based on the suggestions in Nature Protocol „Spheroid-based drug screen: considerations and practical approach“ by J. Friedrich et al. [44]. The preparation of plates coated with an agarose layer consists of three steps:

- Preparation of agarose gel;
- Drying agarose layer;
- Spheroids formation.

2.2.1. Preparation of agarose gel:

1. For one 96-well, flat-bottom cell culture plate, 95 mg of agarose (*Sigma-Aldrich*) and 7 ml of Dulbecco’s Phosphate Buffered Saline (DPBS, *Corning*) solution enriched with calcium and magnesium are needed.
2. Agarose is mixed in DPBS and warmed at 100°C by constant stirring. For this and later steps, a heating plate with a magnetic mixing option and sterile conditions is mandatory.
3. After the agarose solution reaches 100°C, the temperature should be raised to 160°C. The 10-minute timer should be set when the solution starts boiling. After 10 minutes, the temperature should be lowered to 95°C.
4. When the agarose gel is cooled to 95 °C, it is time to add 50 µl to each well. 50 µl of agarose gel is enough to cover the bottom surface and create a concave surface.
5. The plate with agarose gel should be left in the laminar flow cabinet for 30 minutes and moved for the other 30 minutes in the incubator.

Fig. 16 Agarose gel preparation

2.2.2. Spheroids formation

Spheroid formation consists of 3 steps:

Required concentration cell suspension preparation and addition of sufficient volume to each well. Cell suspension is prepared from the collected cells by passaging. To calculate the exact amount of cells required for the formation of spheroids, cells are counted by the hemocytometer. The required amount of cell suspension for spheroids formation is prepared from the cell medium (in the research project RPMI 1640 medium was used) and collected cell suspension. Each well (except the outside layer of wells – they are filled with DPBS to prevent drying of inner wells) is filled with 100 µl of cell suspension.

1. Centrifugation. The plate is placed into a centrifuge for plate centrifugation with set parameters: slow acceleration and deacceleration, 20 minutes of centrifugation, 200 g.

Fig. 17 Special centrifuge for plate centrifugation

2. Incubation. After centrifugation, the plate is wrapped in parafilm to prevent evaporation, and placed in the incubator.

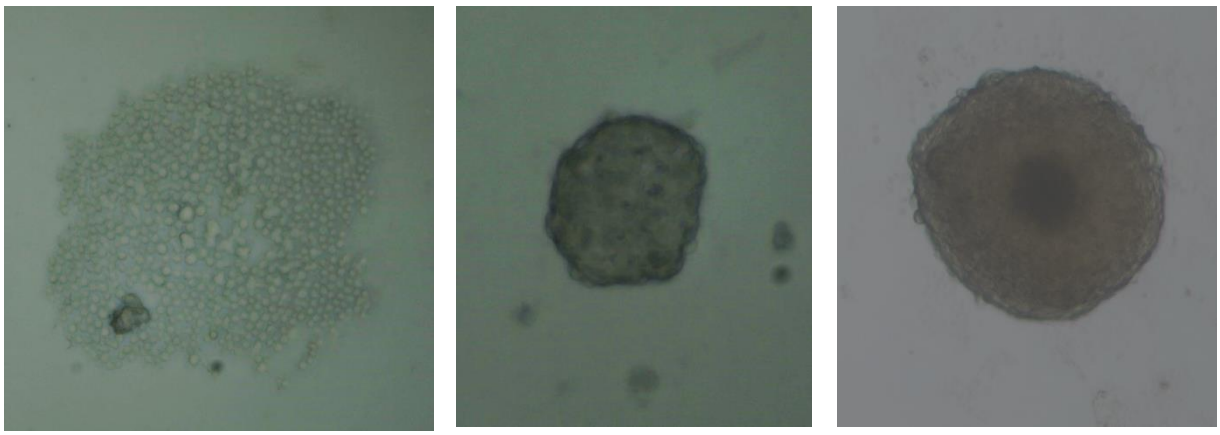

a) b) c)

Fig. 18 Glioblastoma spheroids in different time frames after formation: a) just after centrifugation, b) 24 hours after centrifugation, and c) 7 days after centrifugation

2.3. Treatment

2.3.1. Alpha decay and possible radionuclides for alpha therapy

The nuclei are unstable because the ratio of protons and neutrons differs from the definite range, and to achieve a stable phase, the nuclei undergo a spontaneous transformation that could be called radioactive decay. The decay could appear in a different form; the most probable are alpha, beta decay, or spontaneous fission. During the transformation, the composition of nuclei changes, and it is opposite to gamma decay in that the nuclei composition is not changed, and emission appears due to a transition between energy levels [17].

When the nuclei is heavy, throwing out a stable system of four particles is more energetically profitable than the individual nucleons (for example, alpha particles). The alpha decay is the most typical for heavy elements, with atomic number Z ranging from 82 and atomic mass ranging from 200. When an alpha particle is emitted, the nuclear charge decreases by 2 units and its mass by 4 units [17].

Not all radionuclides can be used for medical purposes. The main characteristics that are important for the selection of radionuclides are activity, half-life, chemical and biological stability, cost, and availability. The radionuclide must be possible to incorporate with pharmaceuticals, and its stability should be long enough to provide treatment. On the other hand, the daughter radionuclides are also important; they can irradiate healthy tissue or be toxic. For targeted alpha therapy, it is also important to know the number and energy of alpha particles emitted throughout decay. A high number of alpha particles and a high energy value will be more efficient for killing malignant cells [7]. The most popular radioisotopes for targeted alpha therapy and their characteristics are listed in Table 2 below.

Table 2 Main parameters of radioisotopes for targeted alpha therapy [7]

Isotope	Half-Life	Max Energy	Emissions Per Decay
^{225}Ac	10.1 d	5.83	4α, 2β-
^{211}At	7.2 h	5.87	1α, 1EC
^{212}Bi	1.01 h	6.09	1α, 1β-
^{213}Bi	45.6 min	5.87	1α, 2β-
^{212}Pb	10.6 h	6.09	1α, 2β-
^{223}Ra	11.4 d	5.87	4α, 2β-
^{224}Ra	3.6 d	8.8	5α, 2β-
^{149}Tb	4.1 h	3.96	1α, 1β+
^{227}Th	18.7 d	6.04	5α, 2β-

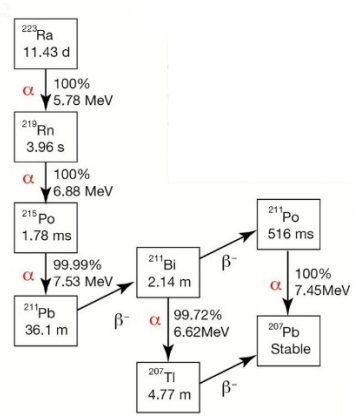

Fig. 19 The decay chain of ^{223}Ra [45]

During the decay process from unstable nuclei of ^{223}Ra to stable nuclei of ^{207}Pb four alpha particles are emitted. These particles have energy from 5.78 MeV to 7.53 MeV. The half-life of ^{223}Ra is long 11.43 days which makes it an ideal candidate for targeted alpha therapy.

In this research project, radionuclides of ^{223}Ra were used as a source of alpha particles. The ^{223}Ra was used in the form of Xofigo® treatment by adjusting the concentration of treatment by diluting it in a cell culture medium for the required specific activity for the experiment.

During the experiment, 50 µl of treatment is added to each well and spheroids are left in the incubator for 24 hours. After 24 hours the medium in the well is replaced 3 times to remove any residue of the treatment.

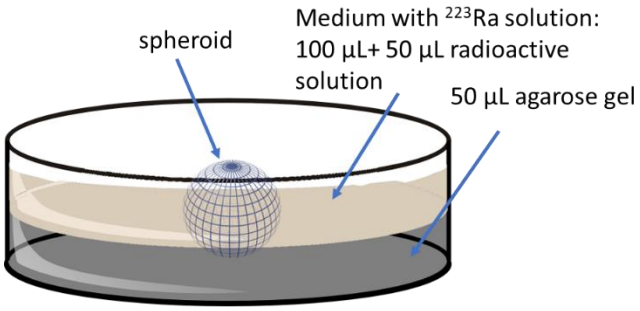

Fig. 20 Schematic view of well in 96 well-plate when treatment solution is added

2.3.2. Specific activity of the treatment measurements

The activities of treatment in the experiment vary from 0.15 kBq/100 µl to 3 kBq/100 µl. To ensure that treatment specific activity is the same for all experiments, a control test step and equipment were established. To measure specific activity in the prepared treatment, NUVIA INSTRUMENTS COMO 170 contamination monitor was used with a 0.25 ml tube holder, which was designed and printed with a 3D printer for these experiments by the medical physicists at the National Cancer Institute (Fig. 21).

Fig. 21 COMO 170 with a tube holder [46]

COMO 170 could be used to measure α or β/γ contamination, and its working principle is based on scintillation. Measurement results are provided in counts per second (cps) and could be measured at a fixed time with automatic or definable smoothing [47].

Scintillation is a result of interaction with ionizing radiation, and then the material (the scintillator) emits flashes of visible light. Then the light is converted to an electrical signal. The light generated in the scintillator by the imparted energy depends on the LET of the charged particle delivering the energy [48].

The reference calibration curve was made by measuring cps values for β particles for the samples of specific activity at points 0.1, 0.375, 0.5, 0.75, 1, 2, and 3 kBq/100 µl. A reference curve is provided in the figure below.

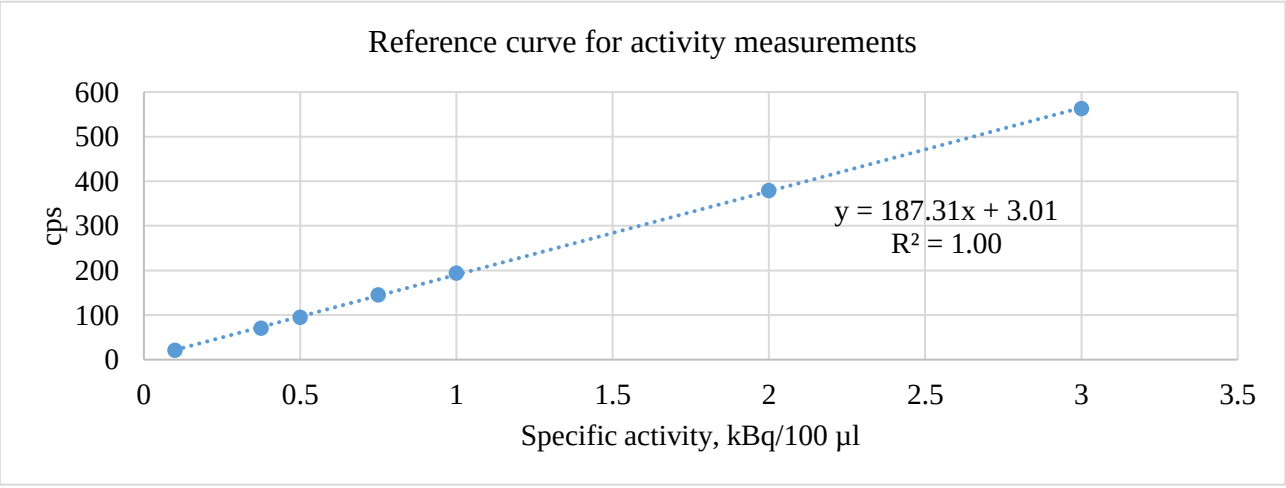

Fig. 22 Reference curve for specific activity measurements

During the experiment, each treatment specific activity is measured three times and the mean value without background value is compared with the reference value.

2.4. Effect evaluation: size measurements and viability test

Spheroid size is monitored in three experiment phases: before treatment, 7 days post-treatment, and 14 days post-treatment. To measure the size of spheroids, each spheroid is photographed with the microscope (magnification 4x, Nikon Eclipse TE2000-U), and later on, each spheroid is measured with the ImageJ program. The diameter of a spheroid is calculated by the equation 4.

$$d = \frac{d_{min} + d_{max}}{2} \tag{4}$$

Where d_{min} is the shortest diameter and d_{max} is the longest diameter of spheroids.

The XTT viability test is performed on the 14th day post-treatment. This test can be used for the quantification of cellular proliferation, viability, and cytotoxicity. This test measures cellular metabolic activity as an indicator of cell viability. During the test, yellow tetrazolium salt (sodium 3'-[1-(phenylaminocarbonyl)- 3,4-tetrazolium]-bis (4-methoxy6-nitro)benzene sulfonic acid hydrate, or XTT), is reduced to formazan dye, which is orange, by the metabolically active cells. The concentration of dye is dependent on the number of living cells that can perform metabolic activity. The amount of dye could be measured by the spectrophotometer. The absorbance of the formazan product is between 450 and 500 nm (in the experiment, it was measured at 490 nm), and the reference wavelength was measured at 630 nm. A microplate reader (*800^{TS}, BioTek*) was used to measure absorbance values for each well [49, 50].

2.5. Timeline of the experiment

Experimental work consists of two parts: the cultivation of cell lines and experiments with spheroids. It is impossible to start an experiment without cell lines, which require attention at least two times per week. During the experiment, the results also depend on the spheroids' well-being, so the medium should be changed at least twice per week to ensure that the cells of the spheroids have enough nutrients. Table 2 provides a full view of the mandatory tasks related to the experiment from the first day of the experiment until the last day. Continuous cell line passaging ensures that a new experiment can be started on the day of cell line passaging.

Table 3 Timeline of experiment

Days	Tasks			
	Cell lines	Spheroids		
		Routine care	Experimental part	Effect evaluation
1	Cell line passaging		Formation	
2				
3				
4	Cell line passaging	Medium renewal		
5				
6				
7				
8	Cell line passaging		Treatment	Imaging
9		Medium renewal		
10				
11	Cell line passaging	Medium renewal		
12				
13				
14				
15	Cell line passaging	Medium renewal	Effect evaluation	Imaging
16				
17				
18	Cell line passaging	Medium renewal		
19				
20				
21	Cell line passaging		Effect evaluation	Imaging and viability test

3. Results

3.1. Treatment of cells with ^{223}Ra (specific activity from 0.15 to 3 kBq/100 µl)

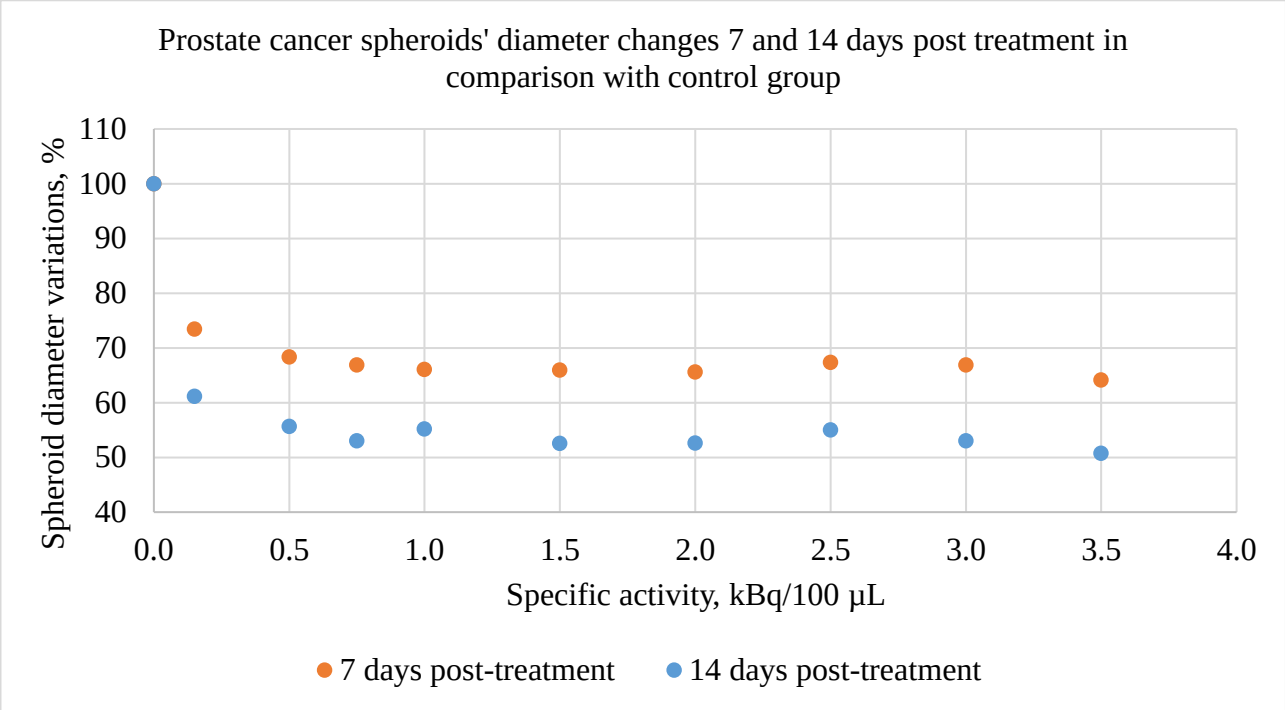

Fig. 23 Relationship of spheroid size and treatment specific activity 7 days and 14 days post-treatment

Prostate cancer spheroids formed from 1000 cells were treated with treatment activities varying from 0,15 kBq/100 µL to 3,5 kBq/100 µL (the response to the treatment is represented in Fig. 23). The purpose of this experiment is to determine the interval of treatment activities at which spheroid diameter changes could be achieved; and to compare results of the viability test, spheroids size changes, and the correlation between. For this experiment, spheroids were formed from 1000 cells, and on the day of treatment, the relative size error was 4.5%.

7 days post-treatment, the highest size reduction was 35.9% from the control group. The highest impact of treatment specific activity was observed with the activities at 0.15 and 0.5 kBq/100 µL; with increasing treatment specific activity, the effect of treatment stayed similar to the effect madded of treatment of 0.5 kBq/100 µL specific activity. The mean spheroid diameter value could be reduced by 26.5% when the specific activity of the treatment is equal to 0.15 kBq/100 µL. When treatment specific activity is equal to 0.5 kBq/100 µL and up to 3.5 kBq/100 µL, the mean diameter value of spheroids varies from 64.1% to 68.3% from the control group, but the difference is relatively small and not significant because the variation of size is similar to the relative error. This experiment shows that the highest potency without changing the treatment plan is achieved with a treatment specific activity of 0.5 kBq/100 µL, and with increasing treatment specific activity, increasing efficacy is not observed.

The results obtained after 14 days post-treatment showed a similar tendency to the results obtained 7 days post-treatment. The tendency of the relationship between treatment specific activity and the mean diameter value stayed the same; just the difference between treated spheroids and the control group is higher: the mean diameter value of spheroids treated at 0.15 kBq/100 µL was reduced by 38.8% (12.3% more when 7 days post-treatment), and with increased treatment specific activity (from

0.5 kBq/100 µL to 3.5 kBq/100 µL), the highest reduction of the mean diameter value by 49.3% was achieved (7 days pos-treatment this value was 35.9%).

This experiment provides a few insights:

In the time of 24 hours, ^{223}Ra is in the media, and alpha particles affect the spheroid from the outside. The highest potency of alpha particles from the outside of the spheroid is achieved with a treatment specific activity of 0.5 kBq/100 µL, and for a higher effect experiment, the treatment concept should be adjusted to check these hypotheses:

- Longer treatment time would be helpful for better ^{223}Ra distribution outside and inside the spheroid, which will allow for deeper penetration of alpha particles inside the spheroid.
- The efficiency of the treatment depends on the depth range of alpha particles. The depth range of alpha particles depends on their energy. By adjusting the alpha particle source according to energy of alpha particles, a higher effect could be achieved at the same incubation time (24 hours).

3.1.1. XTT viability test results

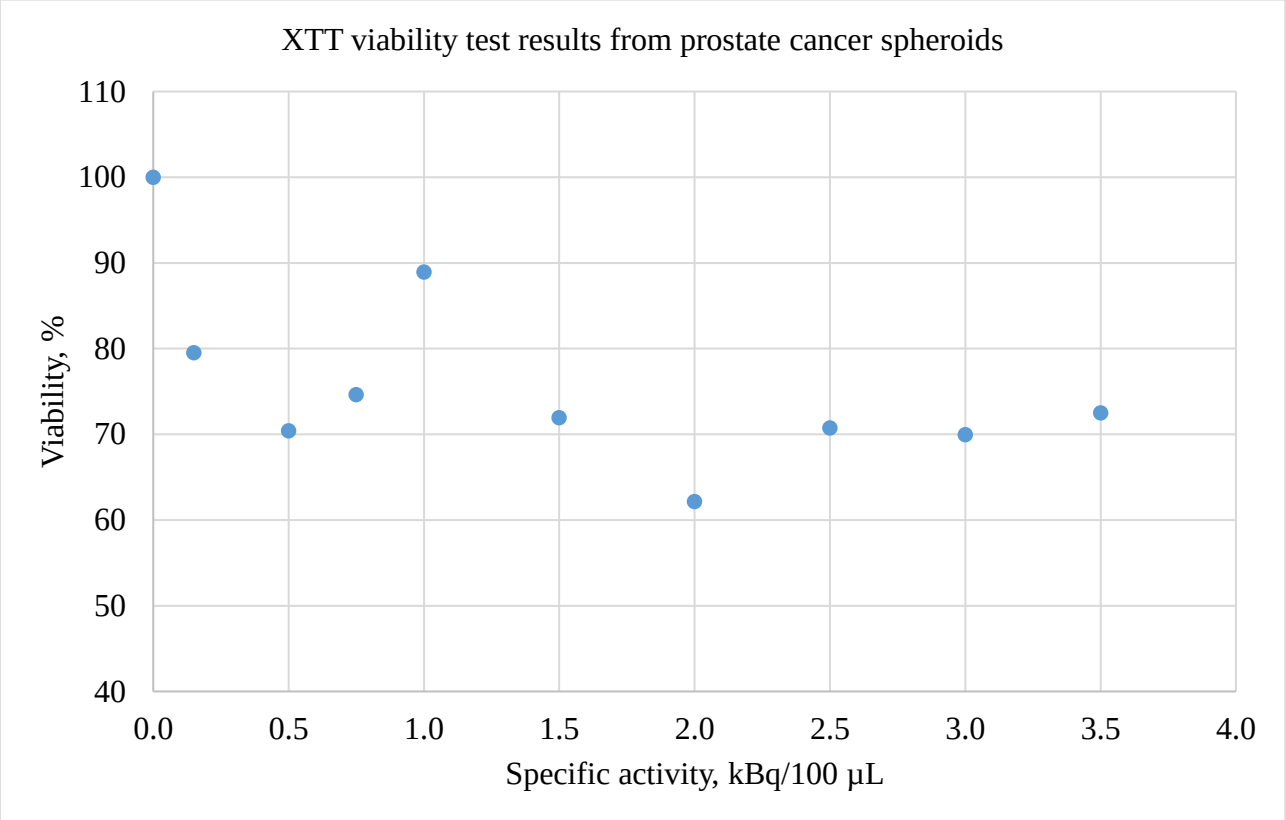

Fig. 24 Results of the viability test

XTT viability test results provided information about treatment toxicity for the spheroids (represented in Fig. 25). The test results correlate with the spheroids' diameter changes from the control group due to the treatment. The Pearson correlation coefficient r is equal to 0.8, and it shows a significant and large positive relationship between XTT results and spheroids' diameter changes. Pearson correlation shows a linear relationship, and in this case, it means that with an increased mean diameter value of the spheroid, the viability value will also increase.

From the results of the XTT test, the tendency of reaction to the treatment is very similar to the spheroids diameter changes: spheroids treated with treatments whose specific activity is equal to 0.15 kBq/100 µl showed reduced viability by 20.5%, while the rest of the spheroids (treated with treatments whose activities vary from 0.5 to 3.5 kBq/100 µl) showed reduced viability by 30%. The diameter changes stayed similar when the treatment specific activity was up to 0.5 kBq/100 µl and this tendency is very similar to the spheroid's diameter changes (represented in fig. 24), just XTT test results showed ~20% higher viability value than the reduction of spheroid size.

In the XTT results, spheroids treated with treatment whose specific activity is equal to 1 kBq/100 µl showed higher viability (88.9%), and spheroids treated with treatment whose specific activity is equal to 2 kBq/100 µl showed smaller viability (62.2%). These results could be associated with the method's sensitivity to the volume of medium in the well. The medium changes in the column (one column is for one type of treatment) proceed with the multichannel pipette, and the small volume differences directly induce changes in the viability test results.

3.1.2. Spheroids growth kinetics

Table 4 Spheroids growth kinetics in comparison with their size on the day of treatment

Specific activity, kBq/100 µL	7 days post-treatment, %	14 days post-treatment, %
0	49.19	87.22
0.15	12.38	17.50
0.5	4.29	6.64
0.75	2.16	1.45
1	1.56	6.16
1.5	-0.26	-0.47
2	0.82	1.41
2.5	0.52	1.91
3	-0.85	-1.44
3.5	-1.65	-1.41

Analysis of spheroid growth kinetics provides useful information on how treatment affects spheroid growth and what effect could be achieved in a long-term experiment. The results are provided in Table 3 above.

The control group showed the highest growth on the 7th day post-treatment; it grew almost 50% of its size on the 7 days. Later on, the growth started to slow down, and the 14th-day post-treatment control group spheroid growth was 87.22% of its size before treatment (38.03% growth in 7 days; in the previous 7 days, the growth was 49.19%). The slowing down in growth could be associated with the increasing necrotic core and decreasing distribution of nutrients, oxygen, and hormones at a deeper level of the spheroid. On the last day of the experiment, the prostate cancer untreated spheroid diameter was approximately 1388.5 µm, and it became impossible to maintain this size of the spheroid. The spheroids, which were treated with the smallest treatment specific activity (0.15 kBq/100 µl), showed reduced growth in both 7 days and 14 days post-treatment. Like with the untreated spheroids, the growth was higher (12.38%) at the first 7 days post-treatment; later 7 days showed reduced growth to 5.12%. Less noticeable growth (maximum growth was 6.64% 14 days

post-treatment) showed spheroids that were treated with the treatment, whose specific activity was equal to 0.5 kBq/100 µl. The growth in the first 7 days was ~2% higher than after 14 days. Treatments with higher specific activity (from 0.5 to 3.5 kBq/100 µl) showed small diameter changes (around ±1%), which could be associated with the relative errors and provide insight that treatments with activities from 0.5 kBq/100 µl prevent spheroids from growing 7 and 14 days post-treatment.

3.2. Treatment of cells with ^{223}Ra (specific activity from 0.1 to 0.75 kBq/100 µl)

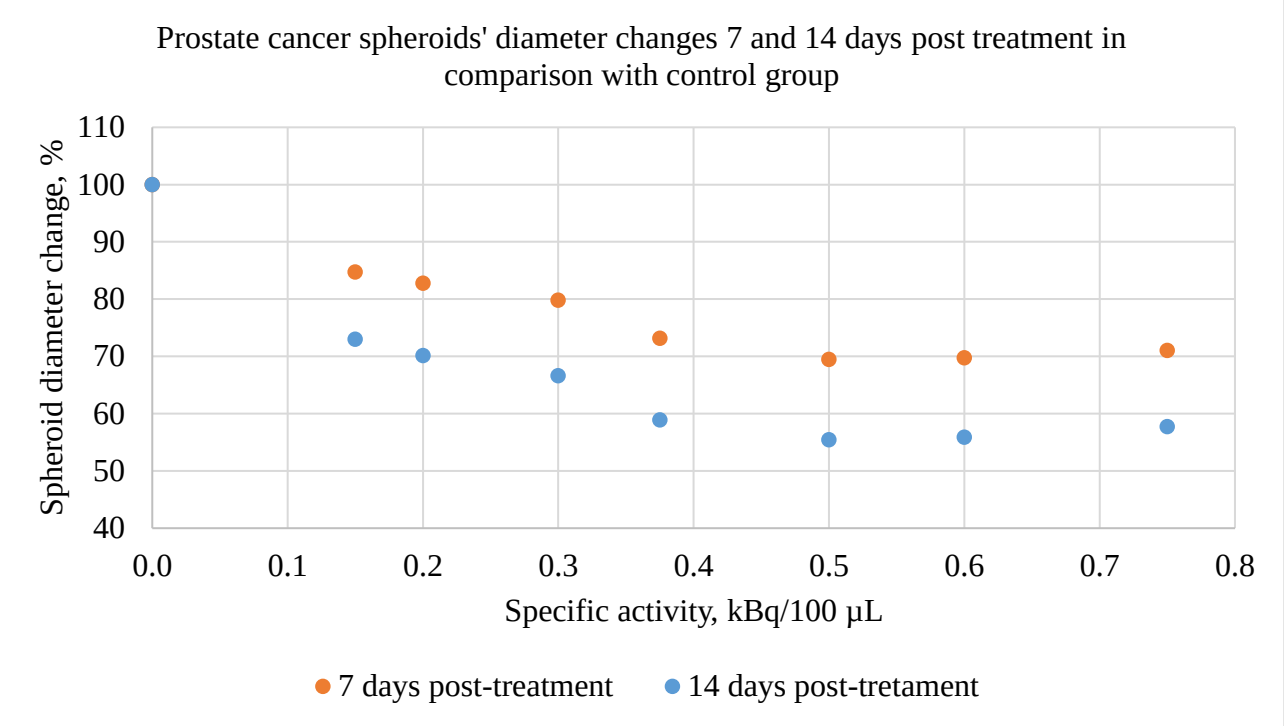

Fig. 25 Relationship of spheroid size and treatment specific activity 7 days and 14 days post-treatment

The purpose of this experiment was to analyze how spheroids react to the treatment with activities at intervals between 0.15 and 0.5 kBq/100 µl (results are represented in fig. 26). The behavior at this interval of activities are important for more precise determination at which treatment specific activity the diameter of spheroid could be reduced by 20%. Spheroids were formed from 1000 cells like in the previous experiment and on the day of treatment, the relative size error was 3.3%. The treatment activities used in this experiment were 0.15, 0.2, 0.25, 0.3, 0.375, 0.425, 0.5, 0.6, and 0.75 kBq/100 µl. The results of the spheroid's relative diameter changes were very similar to the first experiment. Treatments with activities ranging from 0.5 kBq/100 µl had a very similar effect on spheroids' mean diameter values; the increased specific activity in the treatment did not increase the effect on spheroids.

Spheroids treated with activities ranging from 0.15 to 0.5 kBq/100 µl showed an increased diameter size reduction alongside increased treatment specific activity 7 days post-treatment and 14 days post-treatment. The biggest change was observed between activities 0.3 and 0.375 kBq/100 µl; the diameter value of the spheroid was reduced by 6.7% 7 days post-treatment and 7.7% 14 days post-treatment by increasing the treatment specific activity of 0.075 kBq/100 µl. On the other hand, spheroids treated with activities 0.2 and 0.3 showed a reduced reaction to the treatment (diameter was

reduced by 2.9% 7 days post-treatment and 3.5% 14 days post-treatment with an increased 0.1 kBq/100 µl specific activity of treatment).

This experiment confirms that the diameter of the spheroid can be reduced to ~30% 7 days post-treatment and ~45% 14 days post-treatment by using ^{223}Ra treatment. Smaller diameter changes could also be achieved by adapting the specific activity of the treatment to the required percentage of diameter reduction. According to the results, to achieve a 20% diameter reduction 7 days post-treatment, prostate cancer spheroids should be treated with activities from 0.2 to 0.3 kBq/100 µl; 14 days post-treatment, this result could be achieved with activities up to 0.15 kBq/100 µl.

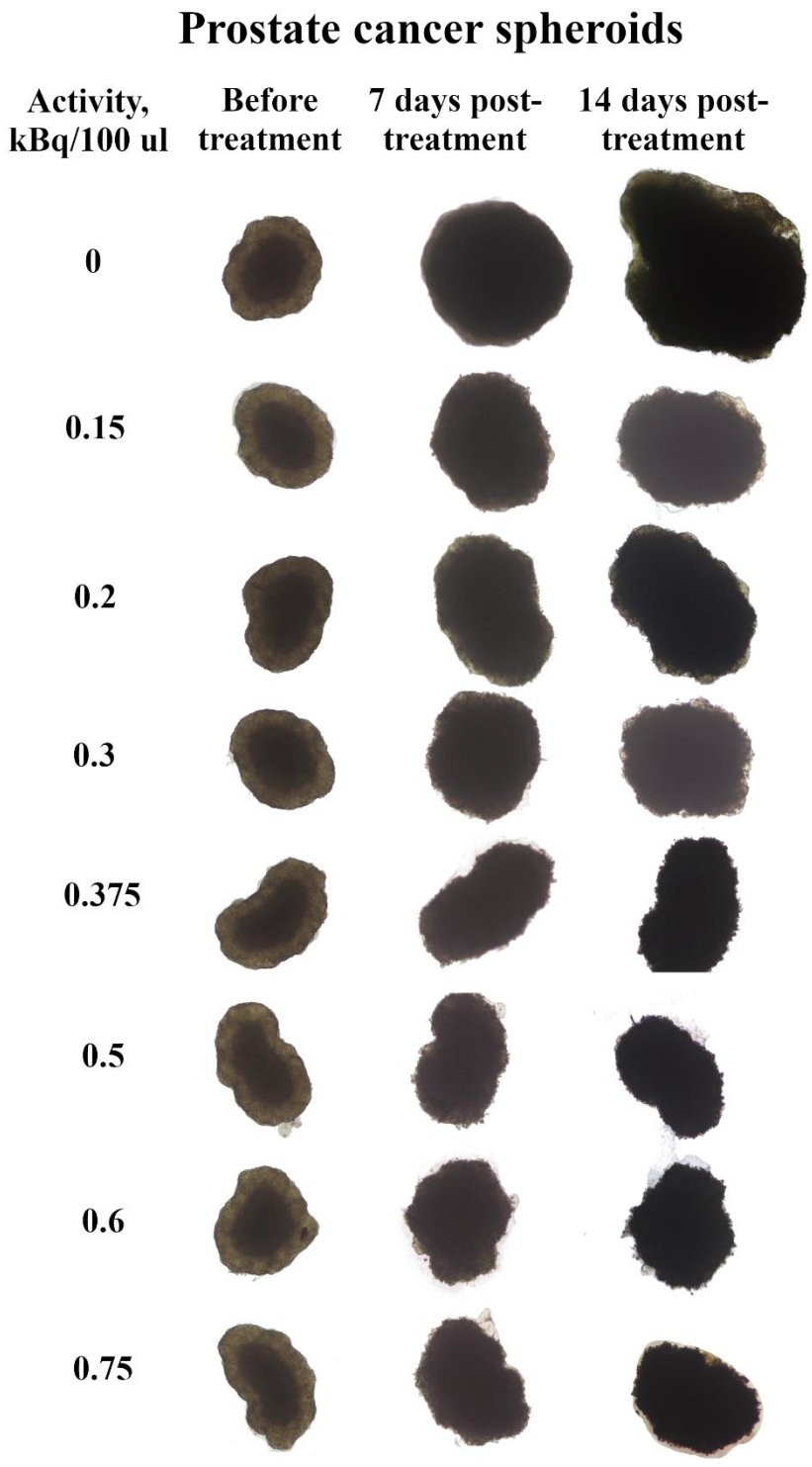

Fig. 26 Prostate cancer spheroids before, 7, and 14 days post-treatment with ^{223}Ra solution

3.3. Treatment of cells with ^{223}Ra: comparison of the effect on different cell types

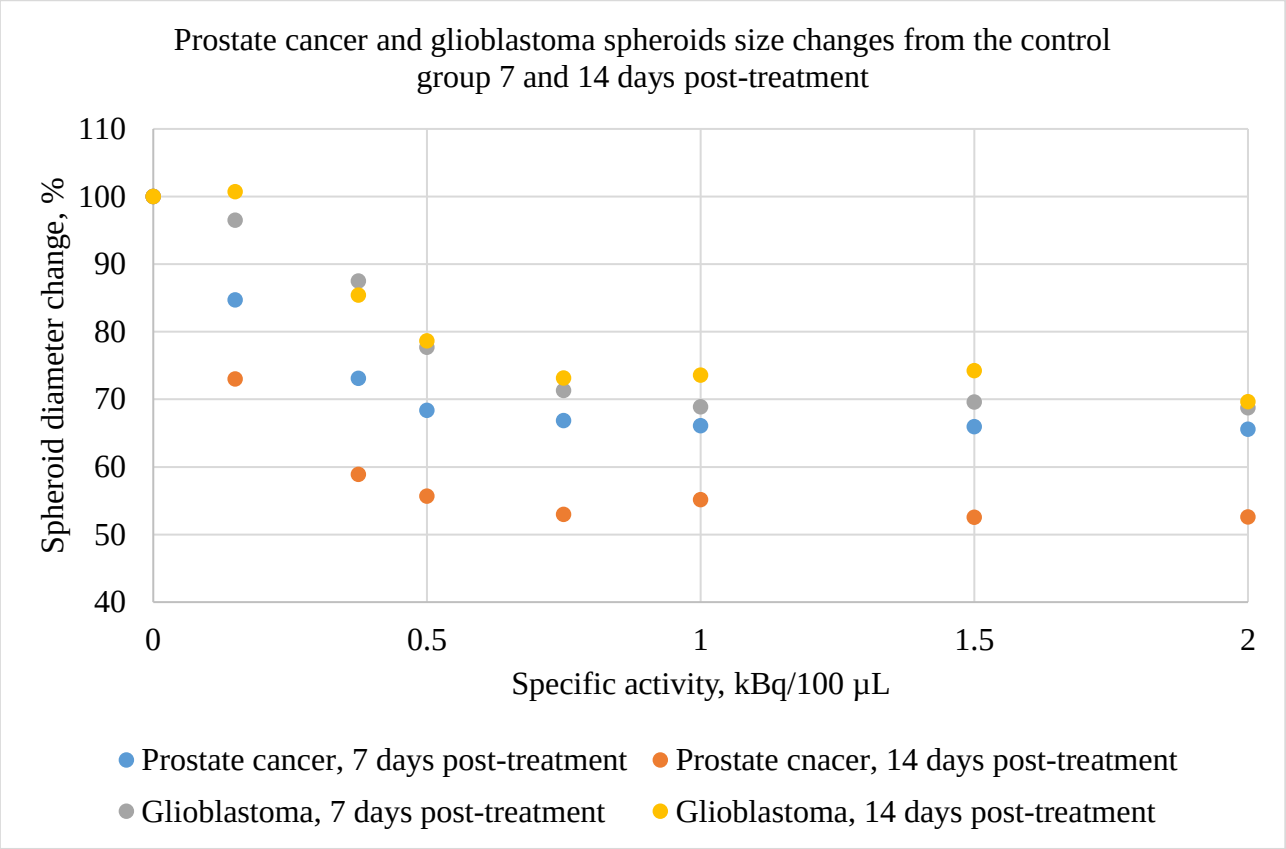

Fig. 27 Relationship of spheroid size and treatment specific activity 7 days and 14 days post-treatment (spheroids of glioblastoma and prostate cancer cell lines)

Two types of cell lines were used in the experiments. The main purpose of using two cell lines was to compare how different types of cells react to the same treatment (results are represented in fig. 27). Spheroids were formed under the same conditions, and the same number of cells were used to form them (spheroids were formed from 1000 cells). Both cell lines have a similar tendency to size-response to the treatment specific activity; prostate cancer and glioblastoma achieved the highest potency of the treatment, whose specific activity was 0.75 kBq/100 µl. Treatments with higher specific activity did not have a stronger effect on spheroid size changes. The biggest differences observed between the two cell lines were sensitivity to the treatment and spheroid growth kinetics (spheroid growth kinetics is revised in the later section for both cell lines).

The glioblastoma cell line showed smaller size changes 7 days and 14 days post-treatment in comparison with the prostate cell line. Glioblastoma spheroids showed almost no changes when the treatment specific activity was 0.15 kBq/100 µL 7 days post-treatment (the mean diameter value was reduced by 3.5%), while the prostate cancer spheroids treated with the same specific activity mean value of diameter was reduced by 15.3% 7 days post-treatment. The same spheroids 14 days post-treatment also showed smaller mean diameter value changes in glioblastoma spheroids; the mean diameter value was almost the same as in the control group (0.7% higher than the control group),

while the mean diameter value of prostate cancer spheroids was reduced by 27%. To achieve a diameter reduction of 20%, glioblastoma spheroids should be treated with treatment activities ranging from 0.375 to 0.5 kBq/100 µL for both 7 days post-treatment and 14 days post-treatment. While prostate cancer spheroids to achieve the same 20% reduction should be treated by the activities from 0.15 to 0.375 kBq/100 µL 7 days post-treatment and to 0.15 kBq/100 µL 14 days post-treatment.

The highest difference in diameter changes due to the treatment between these two lines was observed when the treatment specific activity was equal to 0.15 kBq/100 µL. With the increased specific activity from 0.5 to 2 kBq/100 µL, the difference between the responses to the treatment of both cell lines was more similar: with the treatment specific activity of 0.5 kBq/100 µL, the mean value of prostate cancer spheroids diameter was 9.3% reduced more than glioblastoma spheroids at 7 days post-treatment, and the 14-day post-treatment difference was higher; prostate cancer spheroids showed 22.9% higher mean diameter value reduction than glioblastoma spheroids. With higher treatment activities (from 0.75 to 2 kBq/100 µl), the difference in reaction to the treatment stayed similar: 7 days post-treatment, prostate cancer spheroids mean diameter values were from 4.4% to 2.8% smaller than glioblastoma spheroids; the 14-day post-treatment difference varied from 21.7% to 17%. This result showed that the glioblastoma cell line is more resistant to the treatment, and the difference in reaction is highest when small-specific activity treatment is applied. With increased activity, the difference between cell lines reaction tends to decrease and reaches 2.8% at treatment activity 1 kBq/100 µL 7 days post-treatment, and 17% at activity 2 kBq/100 µL 14 days post-treatment.

3.3.1. XTT viability tests

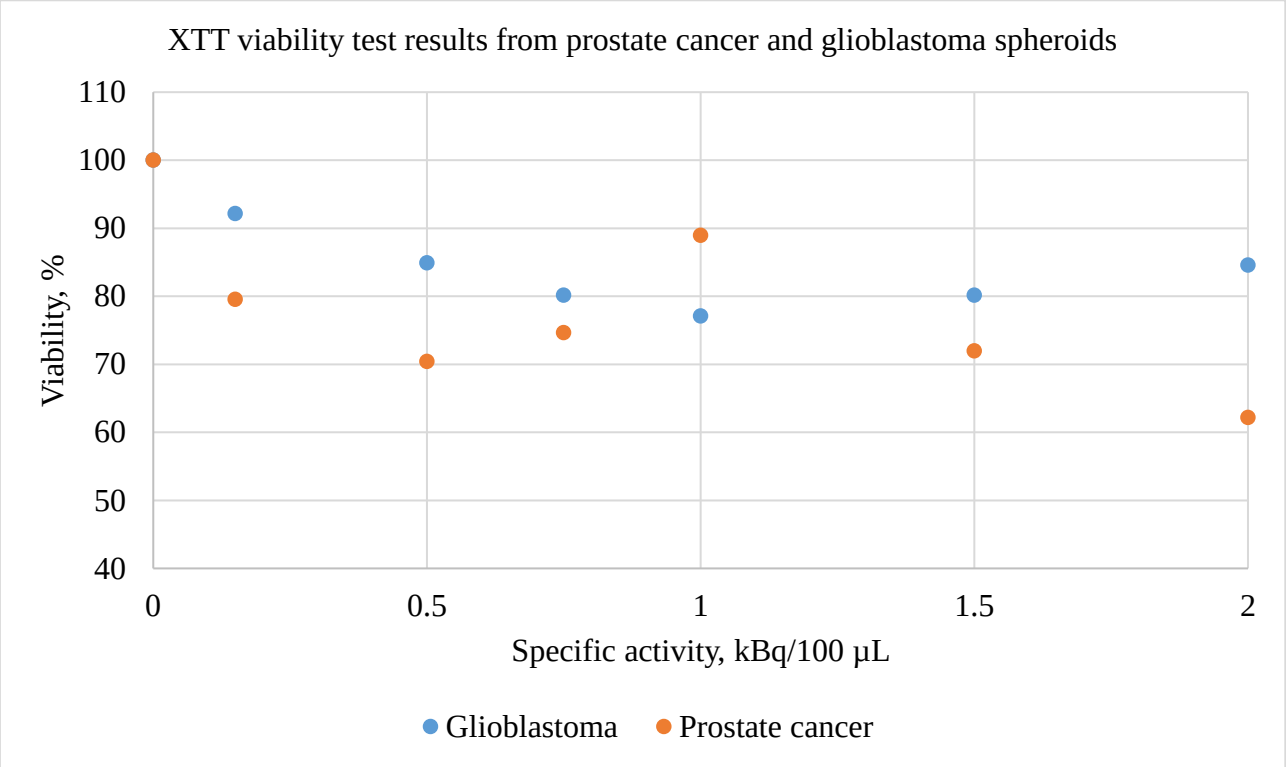

Fig. 28 Results of the viability test

14 days post-treatment, the XTT viability test was performed for both cell lines. Both cell lines showed a significant positive relationship between the results of viability tests and relative spheroids

diameter value. The Pearson correlation coefficient for the glioblastoma cell line is 0.88; for prostate cancer, it is 0.8. For both cell lines, results from the viability test showed higher viability in comparison with the mean diameter value. The glioblastoma cell line showed on average 4% higher viability, and the prostate cancer cell line showed on average 17% increased viability in comparison with diameter changes. Despite the differences, there is a significant relationship between mean diameter values and results from viability tests, and it confirms that spheroidal size assessment could be used as a tool for the effect of spheroidal viability evaluation, and the results provided by this method will not be highly impacted by the cell line. On the other side, this test provided information that the mean difference between the results of the viability test and the mean value of spheroid diameter could be impacted by the cell line, and with more tight spheroids (like the glioblastoma cell line), the difference could be smaller than with less tight spheroids (the prostate cancer cell line).

Glioblastoma spheroid	Prostate cancer spheroid

7 days post-formation (before treatment)

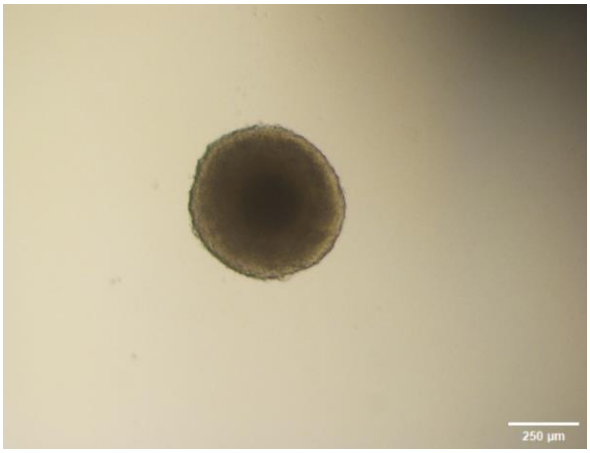

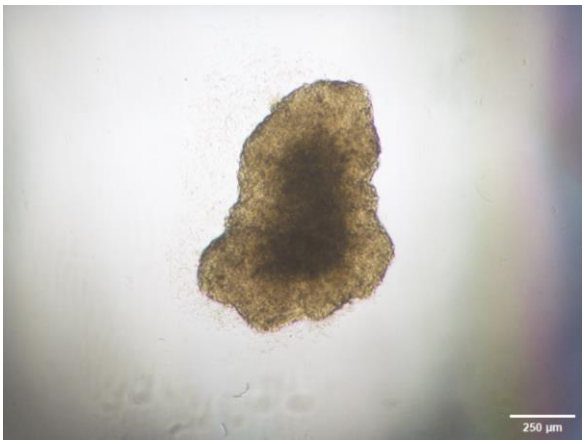

7 days post-treatment (0.15 kBq/100 µL)

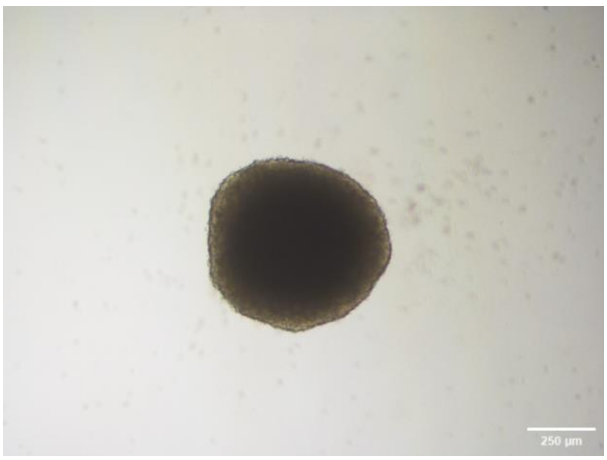

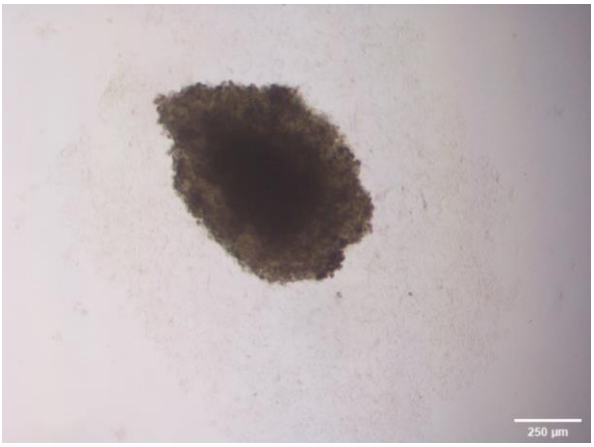

7 days post-treatment (0.75 kBq/100 µL)

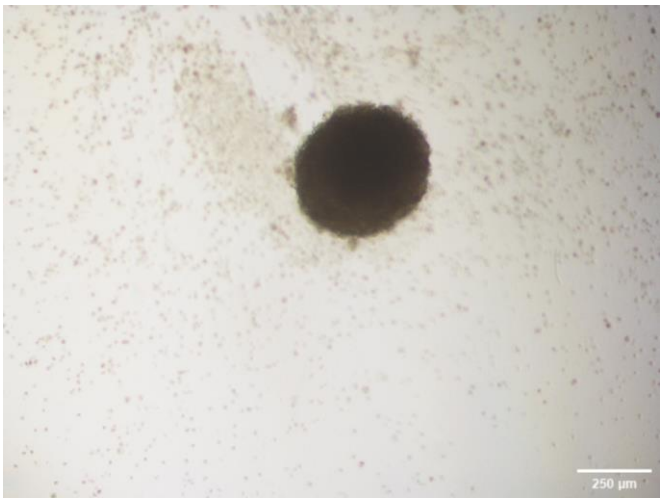

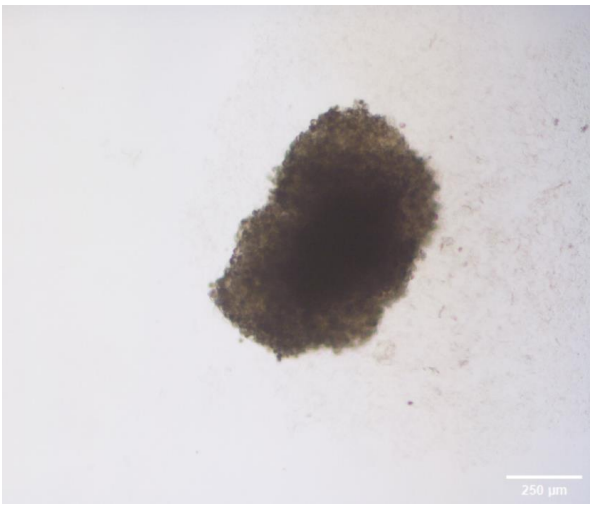

14 days post-treatment (0.15 kBq/100 µL)

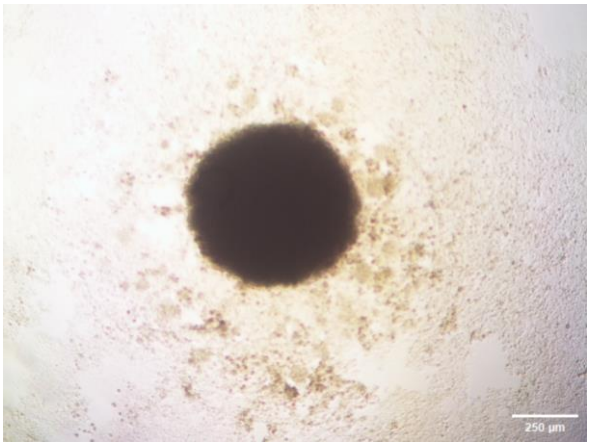

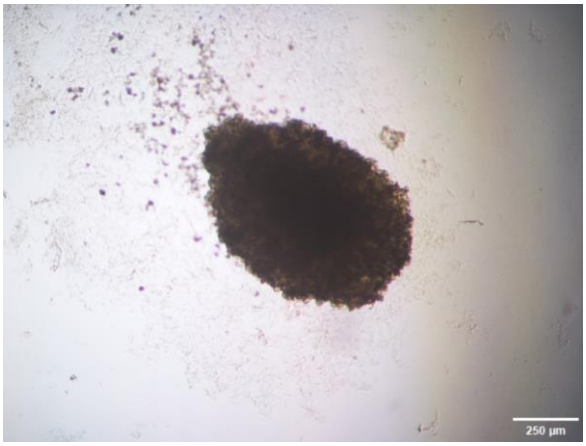

14 days post-treatment (0.75 kBq/100 µL)

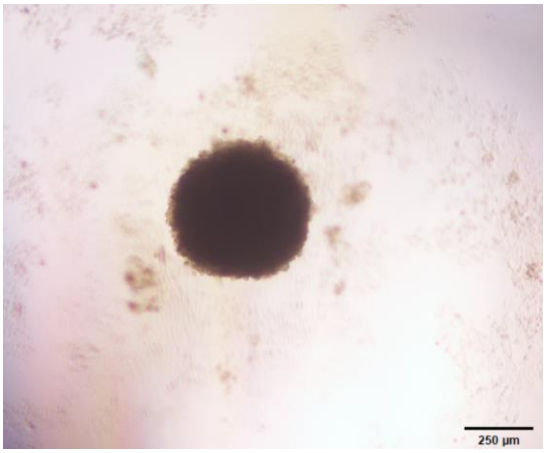

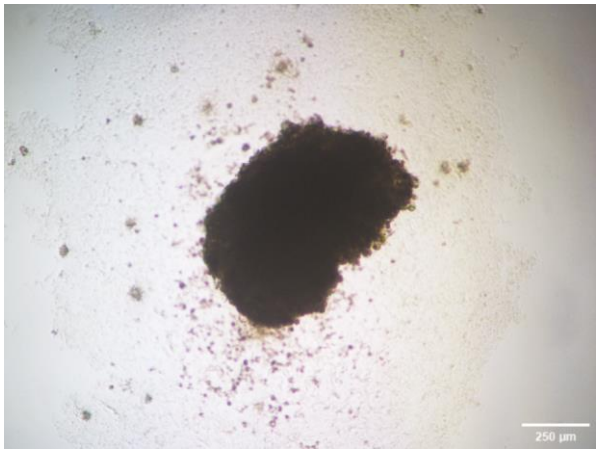

3.3.2. Spheroids growth kinetics

Table 5 Comparison of the growth kinetics of prostate cancer and glioblastoma spheroids with their size on the day of treatment.

Activity, kBq/100 µL	7 days post-treatment, %	14 days post-treatment, %

	Prostate cancer	Glioblastoma	Prostate cancer	Glioblastoma
0	49.19	18.83	87.22	22.52
0.15	12.38	13.11	17.50	21.66
0.5	4.30	-7.15	6.64	-3.14
0.75	2.16	-15.67	1.45	-10.36
1	1.56	-21.5	6.16	-12.10
1.5	-0.26	-18.79	-048	-10.81
2	0.82	-19.21	1.41	-15.58

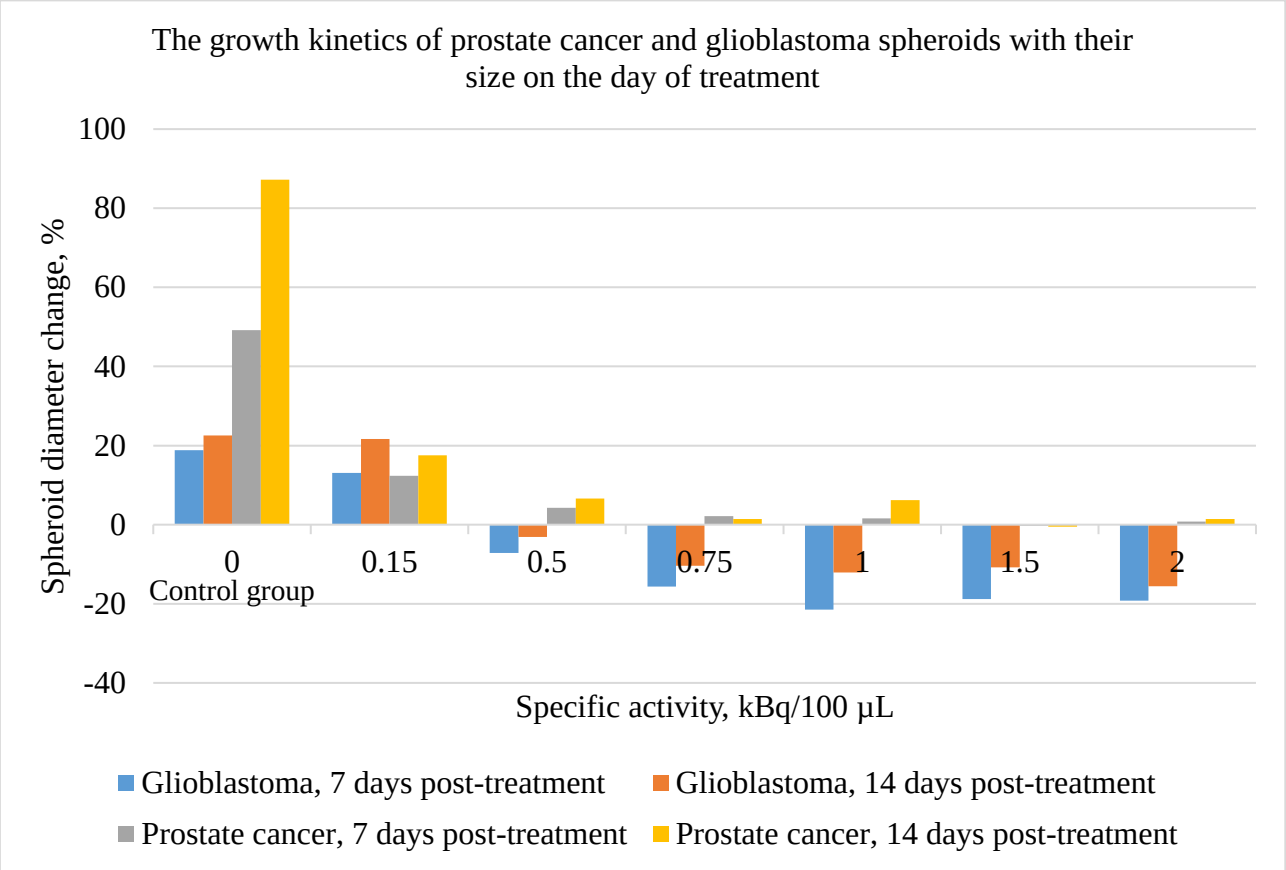

Fig. 29 Glioblastoma and prostate cancer spheroids growth kinetics 7 and 14 days post-treatment

The control group size changes of spheroids are more pronounced in the prostate cancer cell line in comparison with the glioblastoma cell line. Prostate cancer showed more than twice as much growth on the 7th day post-treatment and more than four times on the 14th day post-treatment. Glioblastoma spheroids treated with treatment activity of 0.15 kBq/100 µL had a similar size to the control group; 7 days post-treatment, the mean diameter value was reduced by 5.72% and 0.85% 14 days post-treatment, while the prostate cancer cell line showed a mean diameter value reduction of 36.81% 7 days post-treatment and 69.72% 14 days post-treatment with the same treatment activity. From the treatment activity of 0.5 kBq/100 µL, glioblastoma spheroids stopped growing and started to decrease (the highest decrease in size was observed when treatment activity was 1 kBq/100 µL 7 days post-treatment and when treatment activity was 2 kBq/100 µL 14 days post-treatment). The difference in the decrease in size between treatment activities from 1 kBq/100 µL to 2 kBq/100 µL is relatively small (relative diameter error ± 6%) and fits into the error margins. Prostate cancer spheroids showed increased size and growth with all treatment activities. The activity of treatment reduced growth (the

highest relative diameter reduction was observed in spheroids treated with 0.15 kBq/100 µL), but spheroids even treated with high activities (0.75 and more kBq/100 µL) did not start to decrease in size like glioblastoma spheroids. When treatment activity was from 0.75 kBq/100 µL to 2 kBq/100 µL, spheroids stopped growing, and the results were very similar despite increased activity (the variation was relatively small and varied around 6%).

Total differences between the largest spheroids (in both cases, it is a control group) and the smallest spheroids (treated with 1 kBq/100 µL and higher activities) for the glioblastoma cell line were 40.33% 7 days post-treatment and 38.09% 14 days post-treatment; for the prostate cancer cell line, the differences were 49.45% 7 days post-treatment and 87.70% 14 days post-treatment. The glioblastoma cell line showed a smaller response in size changes due to the treatment; a higher response was also observed 7 days post-treatment, while the prostate cancer cell line showed a higher difference in both experiment time points, and with time the effect on growth also increased. These results show that prostate cancer spheroids are more responsive (more sensitive) to the treatment, and the influence of the treatment on spheroid growth is higher than for glioblastoma cell line spheroids.

3.4. Treatment of cells with ^{223}Ra: comparison of the effect on different spheroid size

The purpose of this experiment was to analyze how spheroid size can influence the effect of treatment. For the experiment, two different cell lines of spheroids from 500 and 2000 cells were formed (results are represented in figures 29 and 30).

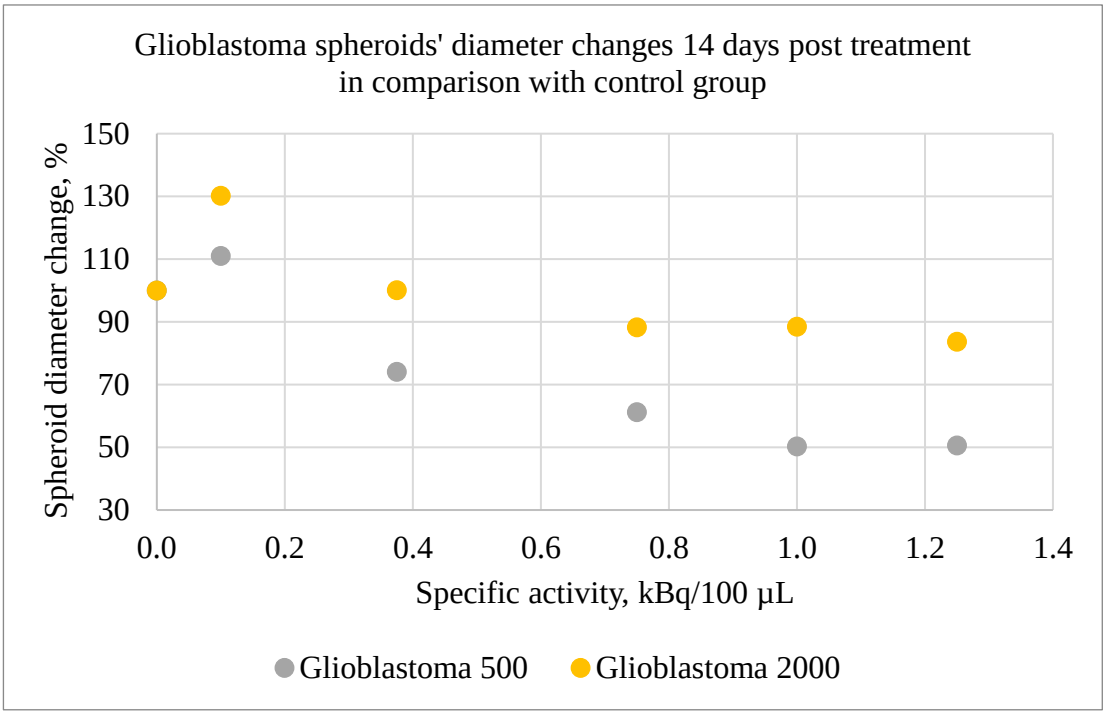

Fig. 30 Different size spheroids (formed from 500 and 200 cells) reaction to the treatment 7 days and 14 days post-treatment (glioblastoma spheroids)

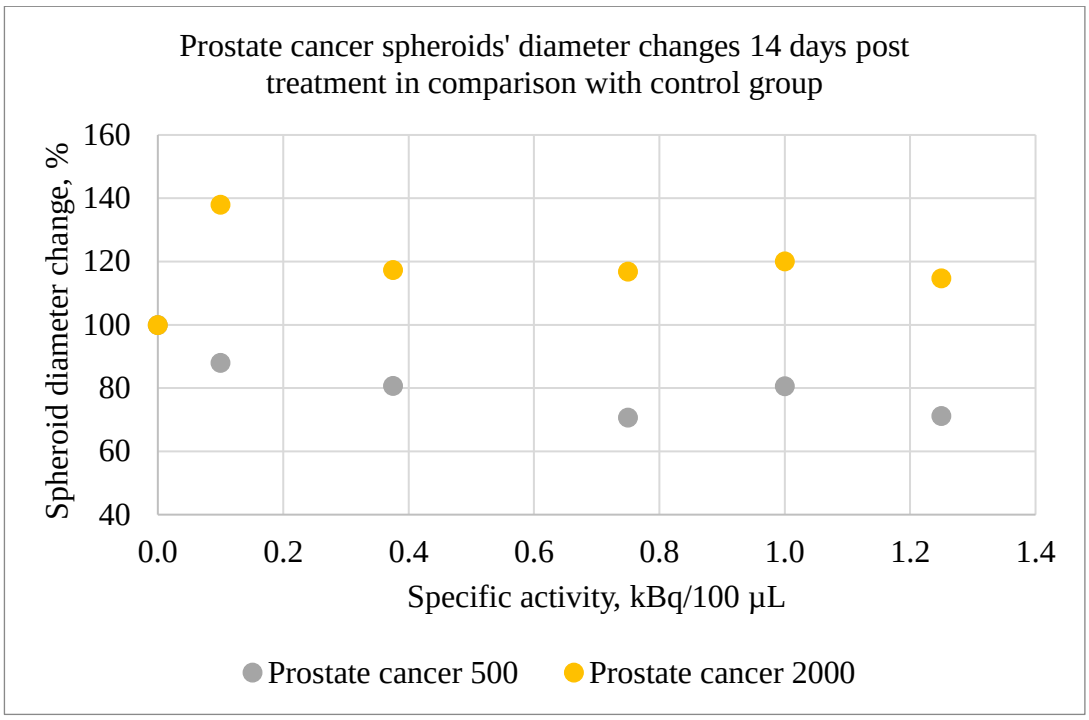

Fig. 31 Different size spheroids (formed from 500 and 200 cells) reaction to the treatment 7 days and 14 days post-treatment (prostate cancer spheroids)

Both cell lines (prostate cancer and glioblastoma) showed increased sensitivity to the treatments when spheroids were smaller in size (formed from 500 cells). The mean value of the difference in reaction to the treatment between glioblastoma spheroids formed from 2000 cells and spheroids formed from 500 cells is 28.7%. This means that smaller spheroids of glioblastoma tend to be 28.7% more sensitive in comparison with bigger spheroids formed from 2000 cells. 28.7% is the mean value of all differences in the whole range of treatment activities, but the difference between spheroids formed from 2000 cells and 500 cells with increased specific activity difference also increases till achieves 38.25% at the treatment specific activity is equal to 1 kBq/100 µl.

Prostate cancer line spheroids like spheroids formed from glioblastoma cells showed higher sensitivity to the treatment when spheroids' size was smaller. On the other hand, the mean value of the difference between bigger spheroids (formed from 2000 cells) and smaller ones (formed from 500 cells) is higher than glioblastoma spheroids – 43.1% (glioblastoma spheroids – 28.7%), that shows that the prostate cancer spheroids are more sensitive to the size changes than glioblastoma.

On the other hand, overall sensitivity to the treatment with ^{223}Ra showed a higher effect on glioblastoma spheroids, which was different from spheroids formed from 1000 cells. It is also interesting that spheroids formed from 2000 cells are bigger than the control group, especially prostate cancer spheroids but the XTT viability test showed that the viability of spheroids is around 46%. This could be related to the spheroid degradation process when cells start to separate from the spheroid and the size of a spheroid is increased due to weak connections between cells. Due to the high diameter value (almost 1 mm), it is impossible to ensure a proper environment for spheroid growth, so this size of spheroid is not very suitable to use for the experiment protocol used in this study. Glioblastoma spheroids are smaller and form more compact spheroids than the prostate cancer cell line. This property could influence the results of the experiment.

3.5. Irradiation with photons

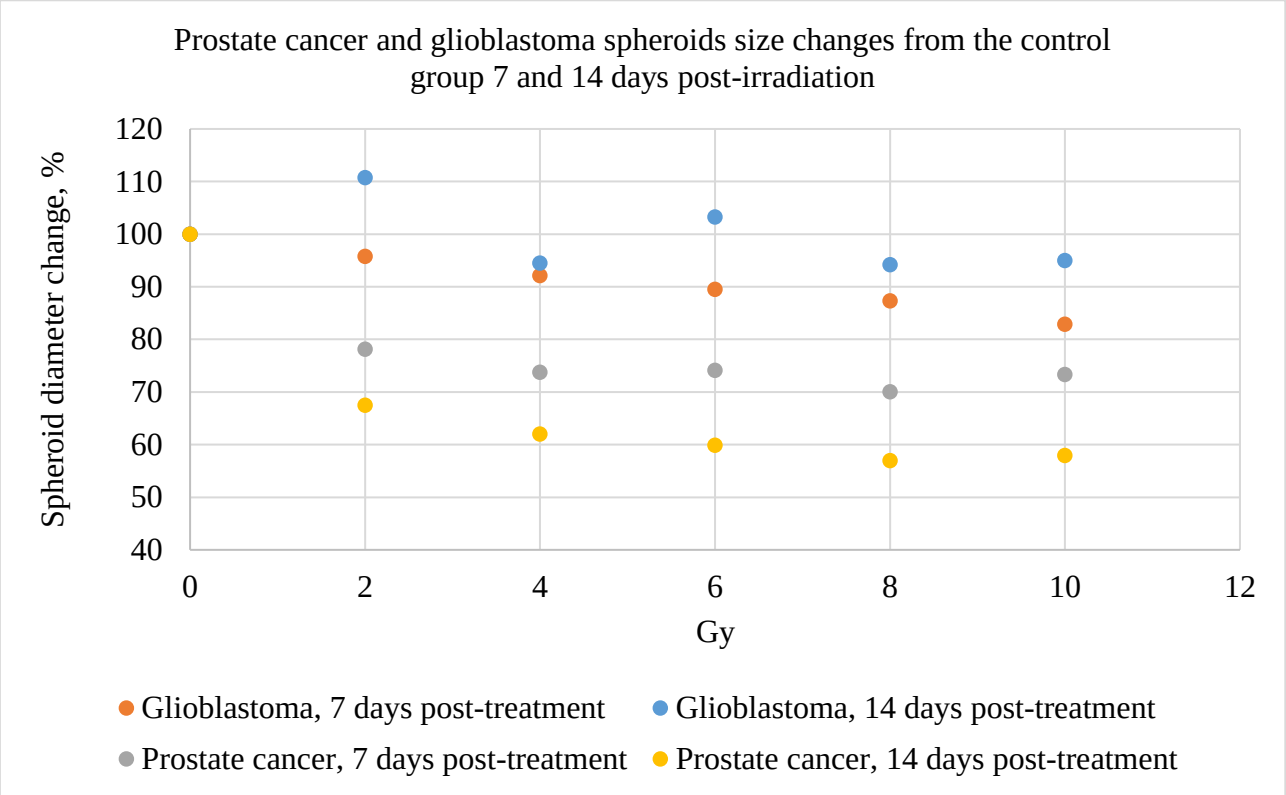

Fig. 32 Glioblastoma and prostate cancer spheroids diameter changes due to irradiation of 6 MeV energy photons

To compare the effect of different types of ionizing radiation on spheroids and distinguish which reactions are related to the cell line but not to the treatment, glioblastoma, and prostate cancer spheroids were irradiated with the photons of 6 MeV energy by Varian True Beam linear accelerator. Irradiation dose varied from 2 to 10 Gy. The procedure of cultivation was the same – size assessment was made in three experimental time points – on the day of the treatment, 7 days post-treatment, and 14 days post-treatment.

Both cell lines showed a similar reaction to the irradiation as reacted to the treatment with ^{223}Ra. The Glioblastoma cell line showed a smaller response to the treatment and the difference between the mean value of diameter measured 7 days post-treatment and 14 days post-treatment was smaller than the prostate cancer cell line. The same effect was observed in all experiments with ^{223}Ra so the effect could be related to the particular cell line response. This experiment also shows that the prostate cancer cell line is much more sensitive to the treatment – spheroids irradiated with the same dose appear to be relatively smaller (in comparison with not irradiated ones) than glioblastoma spheroids. This tendency appeared in a whole range of irradiation doses. Prostate cancer spheroids showed an average 15.65% higher decrease in size (from the control group) 7 days post-irradiation and 38.71% 14 days post-irradiation in comparison with glioblastoma cell line spheroids. Prostate cancer spheroids also showed a higher difference between irradiated spheroids and the control group 14 days post-irradiation in comparison with the results of 7 days post-irradiation, while glioblastoma spheroids showed opposite results – the difference between the control group and irradiated spheroids was higher 7 days post-irradiation and 14 days post-irradiation the difference between the control group and irradiated spheroids was smaller.

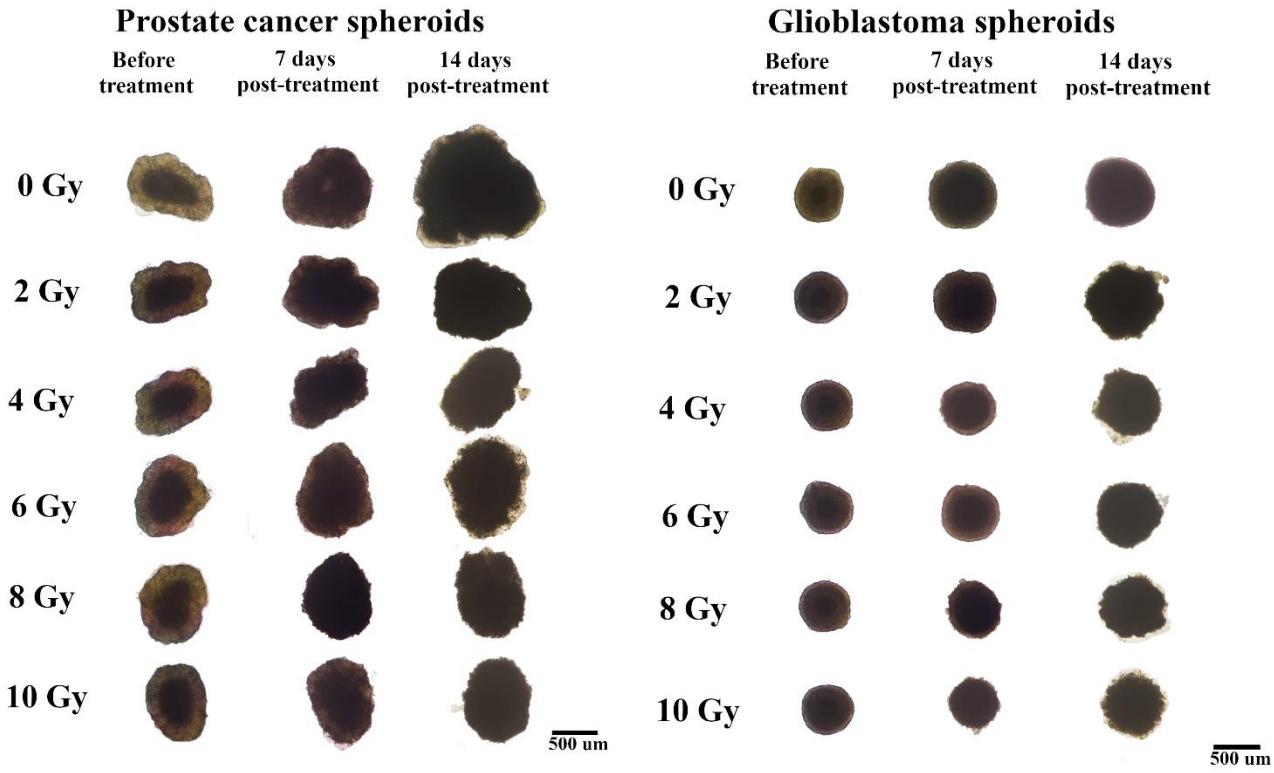

Fig. 33 Glioblastoma and prostate cancer spheroids before, 7, and 14 days post-irradiation 6 MeV energy photons

Irradiation with photons confirms that the response to the treatment not only depends on the type of treatment but also the cell line type. In these experiments, three reactions were observed in all of them and were related to the cell line type:

- Sensitivity to the treatment: glioblastoma showed a reduced response in comparison with the prostate cell line, and it was observed due to smaller size changes due to the treatment or irradiation with photons.
- Prostate cancer spheroids 14 days post-treatment showed an increased diameter reduction in comparison to the diameters 7 days post-treatment, while glioblastoma spheroids 14 days post-treatment had a smaller difference in size between the treated spheroids and the control group (the effect on the diameter value from the treatment had an impact for a shorter time).
- Prostate cancer showed higher relative diameter value differences between results from 7 days post-treatment and 14 days post-treatment, while glioblastoma spheroids showed similar relative diameter size changes from the control group between 7 and 14 days post-treatment.

3.6. Dose calculations using RBE coefficient

According to the literature, the RBE coefficient for ^{223}Ra is equal to 5.6 [51]. The RBE coefficient is calculated by equation 3.

$$RBE(x) = \frac{D_r(x)}{D_t(x)}$$

Where D_r – absorbed dose from reference radiation; D_t – absorbed dose from tested radiation.

Using this expression, the absorbed dose of tested radiation could be calculated by the equation below, and the effect induced by reference and tested radiation on the spheroid is the same:

$$D_t(x) = D_r(x) \cdot RBE(x) = D_r(x) \cdot 5.6$$

The effect was assessed by the spheroid size changes shown in the figures below (Figures 34 and 35), which represent prostate cancer spheroids diameter changes with different treatment activities and absorbed doses. By using these two curves, the relationship between treatment specific activity and absorbed dose was determined.

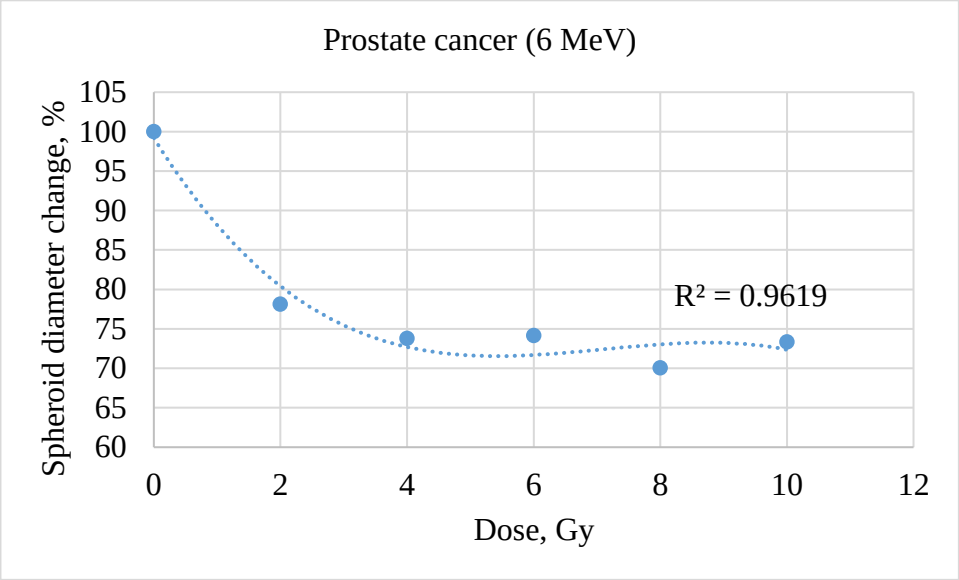

Fig. 34 Prostate cancer spheroids diameter changes due to irradiation of 6 MeV energy photons

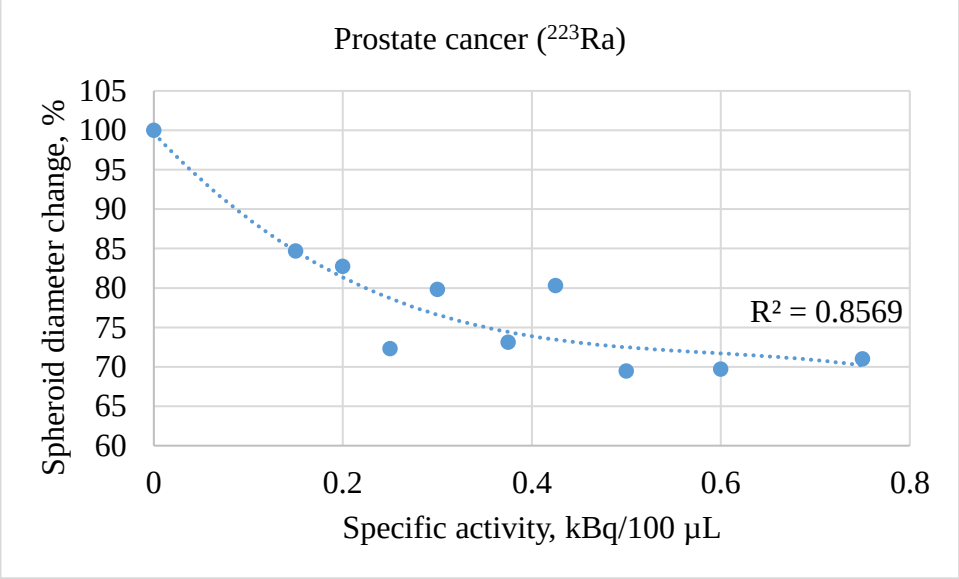

Fig. 35 Prostate cancer spheroids diameter changes due to ^{223}Ra treatment

Equations of trendlines were used to predict the effect on the points at which the experimental point was not made. Because the R^2 value in both relationships (Figures 33 and 34) was higher than 0.85,

this shows that the trendline model predicts values with more than 85% accuracy, which is very important for a more accurate specific activity-dose relationship.

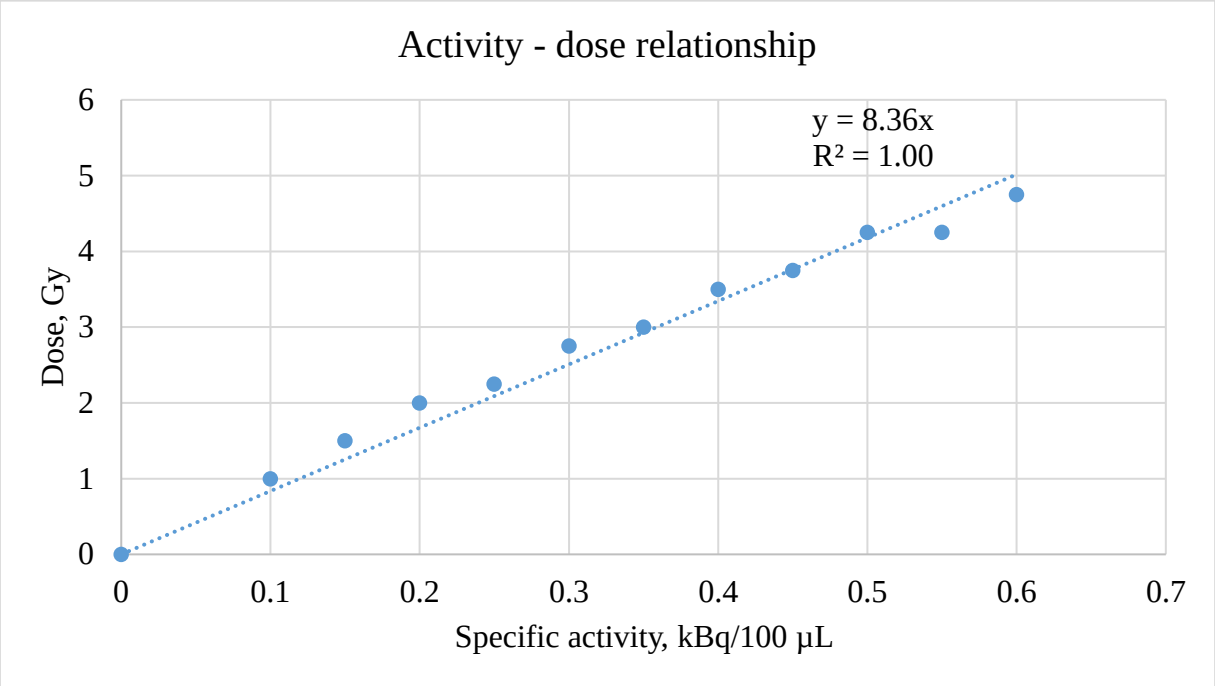

Fig. 36 Calculated specific activity and dose relationship, when RBE of ^{223}Ra is 5.6

The activity-dose relationship (figure 35) could be used as a simplified method to predict the absorbed dose of different ^{223}Ra treatment activities, but it cannot be used as a very accurate method because the absorbed dose depends on various factors: type of radionuclide, time of incubation, and size of the spheroid. In the literature, there are various methods and models to evaluate absorbed doses, but much more complex methods require deeper studies and, in most cases, skills in Montecarlo simulations. Due to the suggested method's simplicity, it could be used as a tool for the approximation of the absorbed dose in the experiments before the required skills are gained and models are incorporated.

3.7. Summary of results

During the study, spheroids of different sizes (from 500, 1000, and 2000 cells) were formed from two cell lines: glioblastoma and prostate cancer. The activities of the ^{223}Ra solution were 0.15, 0.2, 0.3, 0.375, 0.5, 0.6, 0.75, 1, 1.25, 1.5, 2, 2.5, 3, and 3.5. Spheroids formed from 1000 cells showed the highest sensitivity to the treatment, while spheroids formed from 2000 cells were the most resistant. This result is associated with the penetration depth of alpha particles; due to the short penetration depth (~65 µm [18]), a smaller proportion of cells are affected in bigger spheroids. Spheroids formed from 500 cells were less sensitive to treatment than spheroids formed from 1000 cells, but this result is associated with better nutrient distribution inside the spheroid, which leads to increased growth and compensation for the death of the outer layer. However, the inner cells of bigger spheroids (formed from 2000 cells) are not supplied with enough nutrients which leads to reduced growth Due to sufficient nutrient delivery spheroids formed from 1000 cells are the most suitable for this kind of experiment. For both cell lines, the highest efficiency of ^{223}Ra solution is achieved at 0.75 kBq/100 µl specific activity of the solution. Increased specific activity at the same treatment protocol does not

have a higher effect on spheroid size. Prostate cancer spheroid size (in comparison with the control group) was 66.07% 7 days post-treatment and 55.16% 14 days post-treatment, glioblastoma spheroids diameter value was 71.31% 7 days post-treatment and 73.14% 14 days post-treatment).

Spheroid growth kinetic is dependent on the cell line. Both cell lines showed growth reduction with increased treatment specific activity. Glioblastoma spheroids started to decrease in size (the growth was negative), and treatment specific activity was 0.5 kBq/100 µl. This effect was observed 7 days post-treatment and 14 days post-treatment. Prostate cancer cell line spheroids expressed twice higher growth in the control group than glioblastoma spheroids, and the smallest value of spheroids growth was -0.26% 7 days post-treatment and -0.48% 14 days post-treatment (glioblastoma spheroids showed -19.21% 7 days post-treatment and -15.58% 14 days post-treatment). Both cell lines showed similar growth kinetic tendencies as in previous experiments: at the specific activity of 0.75 kBq/100 µl, the highest effect is achieved, and with increased specific activity, changes in growth kinetics are not significant.

Glioblastoma spheroids (formed from 1000 cells) treated with the specific activity of 0.375 kBq/100 µl showed a size reduction of 14.5% 7 days post-treatment and 12.5% 14 days post-treatment. With the treatment specific activity of 0.5 kBq/100 µl, the size of glioblastoma spheroids was reduced by 21.38% 7 days post-treatment and 22.32% 14 days post-treatment. Prostate cancer showed 17.3% size reduction 7 days post-treatment and 29.9% 14 days post-treatment when the treatment specific activity was 0.2 kBq/100 µl. 20% of glioblastoma spheroid size reduction could be achieved with activities ranging from 0.375 to 0.5 kBq/100 µl, while for prostate cancer spheroids, the same size reduction could be achieved with activities ranging from 0.2 kBq/100 µl.

Pearson correlation coefficients were calculated for both cell lines and showed a significant positive relationship between the viability test results and spheroids diameter value. The correlation coefficient for the glioblastoma cell line was 0.88, and for prostate cancer, it was 0.8. The XTT viability test showed decreased viability with increased treatment specific activity. The glioblastoma cell line showed on average 4% higher viability, and the prostate cancer cell line showed on average 17% increased viability in comparison with predicted viability from relative diameter changes. These results show that spheroid viability could be assessed from diameter changes multiplied by the percentage correction factor (the mean value of the difference between spheroids viability and predicted viability from spheroids relative diameter).

Glioblastoma and prostate cancer spheroids formed from 1000 cells were irradiated with 6 MeV photons. Irradiation doses were 2, 4, 6, 8, and 10 Gy. Both cell lines showed size reduction with an increased absorbed dose (with the highest irradiation dose of 10 Gy, glioblastoma spheroids size was reduced by 17.14% 7 days post-irradiation and 4.98% 14 days post-irradiation, prostate cancer showed 26.6% size reduction 7 days post-irradiation and 42.04% 14 days post-irradiation). On average Prostate cancer spheroids showed a 15.65% higher decrease in size (from the control group) 7 days post-irradiation and 38.71% 14 days post-irradiation in comparison with glioblastoma cell line spheroids.

Absorbed doses from different specific activities of ^{223}Ra solutions were calculated based on the RBE value for ^{223}Ra (RBE(^{223}Ra) = 5.6), prostate cancer spheroids size changes due to irradiation with gamma and alpha radiation. The RBE value and reference dose relationship could be used to determine the absorbed dose from different activities of ^{223}Ra solution. This method could be applied

for spheroids whose size is similar to the prostate cancer spheroids, whose data was used for calculations, and for the ^{223}Ra radionuclide.

Conclusions

1. Different cell cultures respond differently to applied alpha activities. The most pronounced effect of alpha particle irradiation is observed on 1000 cell spheroids treated with a specific activity of 0.75 kBq/100 µl.
2. 20% of glioblastoma spheroid size reduction could be achieved after treatment with the specific activity of 0.5 kBq/100 µl, while for prostate cancer spheroids, the same size reduction could be achieved after treatment with the specific activities from 0.15 to 0.2 kBq/100 µl.
3. The size of spheroid‘s diameter correlates with viability, thus indicating that spheroid‘s diameter measurements allow for the evaluation of cell viability using a correction factor.
4. Different irradiation doses have different impact on different cell cultures. As the absorbed dose increases, its impact on spheroids also increases.
5. The absorbed dose can be derived from alpha specific activity by multiplying it by the coefficient 8.36.

Recommendations:

- For optimal nutrient delivery, it is recommended to use spheroids formed from 1000 cells for this type of experiment.

- The maximum effect of alpha particles on the spheroid's size is achieved with a treatment specific activity of 0.75 kBq/100 µL. To enhance the effect, consider adjusting the incubation time with the radioactive solution or incorporating different alpha particle emitters.

- Measuring spheroid diameter can serve as a viability indicator; however, it is essential to note the correction factor between viability test results and spheroid diameter changes before using this method.

Acknowledgment

I would like to express my special thanks and gratitude to my supervisor, the head of the Medical Physics Department, Dr. Jonas Venius, at the National Cancer Institute. Thank you for providing the opportunity to explore the world of cells and the future of radiotherapy, for encouraging me to raise questions and find answers, for inspiring me to seek new challenges in the field of science, and for insightful suggestions.

I also want to thank:

Dr. Greta Butkienė for teaching me how to handle cells and for supporting me with invaluable advice on cell culturing and effects evaluation.

Medical Physicist Mindaugas Džiugelis for his invaluable practical contribution and consultation regarding the treatment of radioactive elements.

The staff of the Biomedical Physics Laboratory and the Medical Physics Department for their warm welcome and advice.

The National Cancer Institute for providing the necessary resources and facilities.

List of references

1. HUH, Hyun Do and KIM, Seonghoon. History of Radiation Therapy Technology. *Progress in Medical Physic*. Online. 30 September 2020. Vol. 31, no. 3, p. 124–134. [Accessed 5 May 2024]. DOI 10.14316/PMP.2020.31.3.124.
2. HATCHER-LAMARRE, Jasmine L., SANDERS, Vanessa A., RAHMAN, Mohammed, CUTLER, Cathy S. and FRANCESCONI, Lynn C. Alpha Emitting Nuclides for Targeted Therapy. *Nuclear medicine and biology*. Online. 1 January 2021. Vol. 92, p. 228. [Accessed 3 March 2024]. DOI 10.1016/J.NUCMEDBIO.2020.08.004.
3. MULFORD, Deborah A., SCHEINBERG, David A. and JURCIC, Joseph G. The Promise of Targeted α-Particle Therapy. *Journal of Nuclear Medicine*. 2005. Vol. 46, no. 1 suppl.
4. ZALUTSKY, M. R. and POZZI, O. R. Radioimmunotherapy with alpha-particle emitting radionuclides. *The Quarterly Journal of Nuclear Medicine and Molecular Imaging : Official Publication of the Italian Association of Nuclear Medicine (AIMN) [and] the International Association of Radiopharmacology (IAR), [and] Section of the Society of...* Online. 1 December 2004. Vol. 48, no. 4, p. 289–296. [Accessed 9 March 2024]. Available from: https://europepmc.org/article/MED/15640792
5. ANTONELLI, Francesca. 3D Cell Models in Radiobiology: Improving the Predictive Value of In Vitro Research. *International Journal of Molecular Sciences 2023, Vol. 24, Page 10620*. Online. 25 June 2023. Vol. 24, no. 13, p. 10620. [Accessed 9 March 2024]. DOI 10.3390/IJMS241310620.
6. HALL, Eric J and GIACCIA, Amato J. *Radiobiology for the Radiologist*. . book. Philadelphia : Wolters Kluwer, 2018. ISBN 9781496335418.
7. TAFRESHI, Narges K., DOLIGALSKI, Michael L., TICHACEK, Christopher J., PANDYA, Darpan N., BUDZEVICH, Mikalai M., EL-HADDAD, Ghassan, KHUSHALANI, Nikhil I., MOROS, Eduardo G., MCLAUGHLIN, Mark L., WADAS, Thaddeus J. and MORSE, David L. *Development of targeted alpha particle therapy for solid tumors*. 2019.
8. Deoxyribonucleic Acid (DNA). Online. [Accessed 25 February 2024]. Available from: https://www.genome.gov/genetics-glossary/Deoxyribonucleic-Acid
9. MCMAHON, Stephen Joseph. The linear quadratic model: usage, interpretation and challenges. *Physics in medicine and biology*. Online. 1 January 2018. Vol. 64, no. 1. [Accessed 17 December 2022]. DOI 10.1088/1361-6560/AAF26A.
10. VAN LEEUWEN, C. M., OEI, A. L., CREZEE, J., BEL, A., FRANKEN, N. A.P., STALPERS, L. J.A. and KOK, H. P. The alfa and beta of tumours: A review of parameters of the linear-quadratic model, derived from clinical radiotherapy studies. *Radiation Oncology*. 16 May 2018. Vol. 13, no. 1. DOI 10.1186/s13014-018-1040-z.
11. WANG, Wenjing, LI, Chunyan, QIU, Rui, CHEN, Yizheng, WU, Zhen, ZHANG, Hui and LI, Junli. Modelling of Cellular Survival Following Radiation-Induced DNA Double-Strand Breaks. Online. [Accessed 23 November 2022]. DOI 10.1038/s41598-018-34159-3.
12. ANDISHEH, B., EDGREN, M., BELKIĆ, Dž, MAVROIDIS, P., BRAHME, A. and LIND, B. K. A comparative analysis of radiobiological models for cell surviving fractions at high doses. *Technology in cancer research & treatment*. Online. 2013. Vol. 12, no. 2, p. 183–192. [Accessed 23 November 2022]. DOI 10.7785/TCRT.2012.500306.
13. LIU, L. J., LIU and J., L. Model of cell response to {\alpha}-particle radiation. *arXiv*. Online. 4 July 2012. P. arXiv:1207.1001. [Accessed 20 December 2022]. Available from: https://ui.adsabs.harvard.edu/abs/2012arXiv1207.1001L/abstract

14. SGOUROS, George, ROESKE, John C., MCDEVITT, Michael R., PALM, Stig, ALLEN, Barry J., FISHER, Darrell R., BRILL, A. Bertrand, SONG, Hong, HOWELL, Roger W., AKABANI, Gamal, BOLCH, Wesley E., MEREDITH, Ruby F., WESSELS, Barry W. and ZANZONICO, Pat B. MIRD Pamphlet No. 22 (Abridged): Radiobiology and Dosimetry of α-Particle Emitters for Targeted Radionuclide Therapy. *Journal of Nuclear Medicine*. Online. 1 February 2010. Vol. 51, no. 2, p. 311–328. [Accessed 22 April 2023]. DOI 10.2967/JNUMED.108.058651.
15. RIQUIER, Hélène, WERA, Anne Catherine, HEUSKIN, Anne Catherine, FERON, Olivier, LUCAS, Stéphane and MICHIELS, Carine. Comparison of X-ray and alpha particle effects on a human cancer and endothelial cells: Survival curves and gene expression profiles. *Radiotherapy and Oncology*. 1 March 2013. Vol. 106, no. 3, p. 397–403. DOI 10.1016/J.RADONC.2013.02.017.
16. OBODOVSKIY, Ilya. Passing of Charged Particles Through Matter. *Radiation*. 1 January 2019. P. 103–136. DOI 10.1016/B978-0-444-63979-0.00005-7.
17. OBODOVSKIY, Ilya. Radiation: Fundamentals, applications, risks, and safety. *Radiation: Fundamentals, Applications, Risks, and Safety*. Online. 1 January 2019. P. 1–694. [Accessed 8 April 2024]. DOI 10.1016/C2016-0-02609-8.
18. CEDER, Jens and ELGQVIST, Jörgen. Targeting prostate cancer stem cells with alpha-particle therapy. *Frontiers in Oncology*. 2017. Vol. 6, no. JAN. DOI 10.3389/fonc.2016.00273.
19. DE VINCENTIS, G., GERRITSEN, W., GSCHWEND, J. E., HACKER, M., LEWINGTON, V., O'SULLIVAN, J. M., OYA, M., PACILIO, M., PARKER, C., SHORE, N. and SARTOR, O. Advances in targeted alpha therapy for prostate cancer. *Annals of oncology : official journal of the European Society for Medical Oncology*. Online. 1 November 2019. Vol. 30, no. 11, p. 1728–1739. [Accessed 20 December 2022]. DOI 10.1093/ANNONC/MDZ270.
20. MCDEVITT, M. R., Barendswaard, E., Ma, D., Lai, L., Curcio, M. J., Sgouros, G., Ballangrud, A. M., Yang, W. H., Finn, R. D., Pellegrini, V., Geerlings, M. W., Jr, Lee, M., Brechbiel, M. W., Bander, N. H., Cordon-Cardo, C., & Scheinberg, D. A. *An-Particle Emitting Antibody ([213 Bi]J591) for Radioimmunotherapy of Prostate Cancer* Online. 2000. Available from: http://aacrjournals.org/cancerres/article-pdf/60/21/6095/3250141/ch210006095p.pdf
21. CORROYER-DULMONT, Aurélien, VALABLE, Samuel, FALZONE, Nadia, FRELIN-LABALME, Anne Marie, TIETZ, Ole, TOUTAIN, Jérôme, SOTO, Manuel Sarmiento, DIVOUX, Didier, CHAZALVIEL, Laurent, PÉRÈS, Elodie A., SIBSON, Nicola R., VALLIS, Katherine A. and BERNAUDIN, Myriam. VCAM-1 targeted alpha-particle therapy for early brain metastases. *Neuro-Oncology*. 2020. Vol. 22, no. 3. DOI 10.1093/neuonc/noz169.
22. BALLANGRUD, Åse M., YANG, Wei Hong, PALM, Stig, ENMON, Richard, BORCHARDT, Paul E., PELLEGRINI, Virginia A., MCDEVITT, Michael R., SCHEINBERG, David A. and SGOUROS, George. Alpha-Particle Emitting Atomic Generator (Actinium-225)-Labeled Trastuzumab (Herceptin) Targeting of Breast Cancer SpheroidsEfficacy versus HER2/neu Expression. *Clinical Cancer Research*. Online. 1 July 2004. Vol. 10, no. 13, p. 4489–4497. [Accessed 22 April 2023]. DOI 10.1158/1078-0432.CCR-03-0800.
23. SATTIRAJU, Anirudh, SOLINGAPURAM SAI, Kiran Kumar, XUAN, Ang, PANDYA, Darpan N., ALMAGUEL, Frankis G., WADAS, Thaddeus J., HERPAI, Denise M., DEBINSKI, Waldemar and MINTZ, Akiva. IL13RA2 targeted alpha particle therapy against glioblastomas. *Oncotarget*. 2017. Vol. 8, no. 26. DOI 10.18632/oncotarget.17792.
24. NAVALKISSOOR, Shaunak and GROSSMAN, Ashley. Targeted Alpha Particle Therapy for Neuroendocrine Tumours: The Next Generation of Peptide Receptor Radionuclide Therapy. *Neuroendocrinology*. 2019. Vol. 108, no. 3. DOI 10.1159/000494760.

25. MIRZADEH, Saed. Innovation, Impact, and Strategic Importance of Alpha-Emitting Radionuclides. *Journal of Medical Imaging and Radiation Sciences*. 1 December 2019. Vol. 50, no. 4, p. S21–S25. DOI 10.1016/J.JMIR.2019.07.002.
26. CHAICHAROENAUDOMRUNG, Nipha, KUNHORM, Phongsakorn and NOISA, Parinya. Three-dimensional cell culture systems as an in vitro platform for cancer and stem cell modeling. *World Journal of Stem Cells*. Online. 12 December 2019. Vol. 11, no. 12, p. 1065. [Accessed 22 April 2023]. DOI 10.4252/WJSC.V11.I12.1065.
27. ANTON, Delphine, BURCKEL, Hélène, JOSSET, Elodie and NOEL, Georges. Three-Dimensional Cell Culture: A Breakthrough in Vivo. *International Journal of Molecular Sciences 2015, Vol. 16, Pages 5517-5527*. Online. 11 March 2015. Vol. 16, no. 3, p. 5517–5527. [Accessed 28 May 2023]. DOI 10.3390/IJMS16035517.
28. MUELLER-KLIESER, Wolfgang. Three-dimensional cell cultures: From molecular mechanisms to clinical applications. *American Journal of Physiology - Cell Physiology*. 1997. Vol. 273, no. 4 42-4. DOI 10.1152/AJPCELL.1997.273.4.C1109.
29. BIAŁKOWSKA, Kamila, KOMOROWSKI, Piotr, BRYSZEWSKA, Maria and MIŁOWSKA, Katarzyna. Spheroids as a Type of Three-Dimensional Cell Cultures—Examples of Methods of Preparation and the Most Important Application. *International Journal of Molecular Sciences 2020, Vol. 21, Page 6225*. Online. 28 August 2020. Vol. 21, no. 17, p. 6225. [Accessed 28 May 2023]. DOI 10.3390/IJMS21176225.
30. SUZUKA, Jun, TSUDA, Masumi, WANG, Lei, KOHSAKA, Shinji, KISHIDA, Karin, SEMBA, Shingo, SUGINO, Hirokazu, ABURATANI, Sachiyo, FRAUENLOB, Martin, KUROKAWA, Takayuki, KOJIMA, Shinya, UENO, Toshihide, OHMIYA, Yoshihiro, MANO, Hiroyuki, YASUDA, Kazunori, GONG, Jian Ping and TANAKA, Shinya. Rapid reprogramming of tumour cells into cancer stem cells on double-network hydrogels. *Nature Biomedical Engineering 2021 5:8*. Online. 29 March 2021. Vol. 5, no. 8, p. 914–925. [Accessed 10 March 2024]. DOI 10.1038/s41551-021-00692-2.
31. DOCTOR, Alina, SEIFERT, Verena, ULLRICH, Martin, HAUSER, Sandra and PIETZSCH, Jens. Three-Dimensional Cell Culture Systems in Radiopharmaceutical Cancer Research. *Cancers 2020, Vol. 12, Page 2765*. Online. 25 September 2020. Vol. 12, no. 10, p. 2765. [Accessed 22 April 2023]. DOI 10.3390/CANCERS12102765.
32. DE WITT HAMER, P. C., VAN TILBORG, A. A.G., EIJK, P. P., SMINIA, P., TROOST, D., VAN NOORDEN, C. J.F., YLSTRA, B. and LEENSTRA, S. The genomic profile of human malignant glioma is altered early in primary cell culture and preserved in spheroids. *Oncogene*. Online. 27 March 2008. Vol. 27, no. 14, p. 2091–2096. [Accessed 10 March 2024]. DOI 10.1038/SJ.ONC.1210850.
33. RAITANEN, Julia, BARTA, Bernadette, HACKER, Marcus, GEORG, Dietmar, BALBER, Theresa and MITTERHAUSER, Markus. Comparison of Radiation Response between 2D and 3D Cell Culture Models of Different Human Cancer Cell Lines. *Cells*. Online. 1 February 2023. Vol. 12, no. 3, p. 360. [Accessed 15 January 2024]. DOI 10.3390/CELLS12030360/S1.
34. JUZENIENE, Asta, STENBERG, Vilde Yuli, BRULAND, Øyvind Sverre, REVHEIM, Mona Elisabeth and LARSEN, Roy Hartvig. Dual targeting with 224Ra/212Pb-conjugates for targeted alpha therapy of disseminated cancers: A conceptual approach. *Frontiers in Medicine*. 17 January 2023. Vol. 9, p. 1051825. DOI 10.3389/FMED.2022.1051825/BIBTEX.
35. ZHU, Charles, SEMPKOWSKI, Michelle, HOLLERAN, Timothy, LINZ, Thomas, BERTALAN, Thomas, JOSEFSSON, Anders, BRUCHERTSEIFER, Frank, MORGENSTERN, Alfred and SOFOU, Stavroula. Alpha-particle radiotherapy: For large solid tumors diffusion trumps

targeting. *Biomaterials*. 1 June 2017. Vol. 130, p. 67–75. DOI 10.1016/J.BIOMATERIALS.2017.03.035.
36. SEIFERT, Verena, RICHTER, Susan, BECHMANN, Nicole, BACHMANN, Michael, ZIEGLER, Christian G., PIETZSCH, Jens and ULLRICH, Martin. HIF2alpha-Associated Pseudohypoxia Promotes Radioresistance in Pheochromocytoma: Insights from 3D Models. *Cancers 2021, Vol. 13, Page 385*. Online. 21 January 2021. Vol. 13, no. 3, p. 385. [Accessed 15 January 2024]. DOI 10.3390/CANCERS13030385.
37. ABRAMENKOVS, Andris, HARIRI, Mehran, SPIEGELBERG, Diana, NILSSON, Sten and STENERLÖW, Bo. Ra-223 induces clustered DNA damage and inhibits cell survival in several prostate cancer cell lines. *Translational Oncology*. 1 December 2022. Vol. 26, p. 101543. DOI 10.1016/J.TRANON.2022.101543.
38. JALLOUL, Wael, GHIZDOVAT, Vlad, STOLNICEANU, Cati Raluca, IONESCU, Teodor, GRIEROSU, Irena Cristina, PAVALEANU, Ioana, MOSCALU, Mihaela and STEFANESCU, Cipriana. Targeted Alpha Therapy: All We Need to Know about 225Ac's Physical Characteristics and Production as a Potential Theranostic Radionuclide. *Pharmaceuticals 2023, Vol. 16, Page 1679*. Online. 2 December 2023. Vol. 16, no. 12, p. 1679. [Accessed 9 March 2024]. DOI 10.3390/PH16121679.
39. WEISKIRCHEN, Sabine, SCHRÖDER, Sarah K., BUHL, Eva Miriam and WEISKIRCHEN, Ralf. A Beginner's Guide to Cell Culture: Practical Advice for Preventing Needless Problems. *Cells*. Online. 1 March 2023. Vol. 12, no. 5. [Accessed 27 March 2024]. DOI 10.3390/CELLS12050682.
40. Gibco Cell Culture Basics - LT. Online. [Accessed 27 March 2024]. Available from: https://www.thermofisher.com/tr/en/home/references/gibco-cell-culture-basics.html
41. CLARKE, Sue and DILLON, Janette. The Cell Culture Laboratory. *Animal Cell Culture: Essential Methods*. 30 March 2011. P. 1–31. DOI 10.1002/9780470669815.CH1.
42. KAPAŁCZYŃSKA, Marta, KOLENDA, Tomasz, PRZYBYŁA, Weronika, ZAJĄCZKOWSKA, Maria, TERESIAK, Anna, FILAS, Violetta, IBBS, Matthew, BLIŹNIAK, Renata, ŁUCZEWSKI, Łukasz and LAMPERSKA, Katarzyna. 2D and 3D cell cultures – a comparison of different types of cancer cell cultures. *Archives of Medical Science : AMS*. Online. 2018. Vol. 14, no. 4, p. 910. [Accessed 28 May 2023]. DOI 10.5114/AOMS.2016.63743.
43. SANTINI, M. T., RAINALDI, G. and INDOVINA, P. L. Multicellular tumour spheroids in radiation biology. *http://dx.doi.org/10.1080/095530099139845*. Online. 2009. Vol. 75, no. 7, p. 787–799. [Accessed 22 April 2023]. DOI 10.1080/095530099139845.
44. FRIEDRICH, Juergen, SEIDEL, Claudia, EBNER, Reinhard and KUNZ-SCHUGHART, Leoni A. Spheroid-based drug screen: considerations and practical approach. *Nature Protocols 2009 4:3*. Online. 12 February 2009. Vol. 4, no. 3, p. 309–324. [Accessed 8 April 2024]. DOI 10.1038/nprot.2008.226.
45. ABOU, Diane S., ULMERT, David, DOUCET, Michele, HOBBS, Robert F., RIDDLE, Ryan C. and THOREK, Daniel L.J. Whole-Body and Microenvironmental Localization of Radium-223 in Naïve and Mouse Models of Prostate Cancer Metastasis. *Journal of the National Cancer Institute*. Online. 1 May 2016. Vol. 108, no. 5. [Accessed 9 April 2024]. DOI 10.1093/JNCI/DJV380.
46. VALIUKEVIČIŪTĖ, Džiugilė, BUTKIENĖ, Greta, DŽIUGELIS, Mindaugas, TIŠKEVIČIUS, Sigitas, GRIGALAVIČIUS, Mantas and VENIUS, Jonas. The effect of different activities of alpha particles on glioblastoma 3D cell culture. *Medical physics in the Baltic states: proceedings of the 16th international conference on medical physics, Kaunas, Lithuania, 9-11 November 2023*. 2023. P. 153–156.

47. CoMo 170: hand-held contamination monitor - NUVIATech. Online. [Accessed 10 April 2024]. Available from: https://www.nuviatech-instruments.com/product/nuhls-como-170-zs/
48. ATTIX, Frank Herbert. Introduction to Radiological Physics and Radiation Dosimetry. *Introduction to Radiological Physics and Radiation Dosimetry*. Online. 19 November 1986. [Accessed 11 April 2024]. DOI 10.1002/9783527617135.
49. Protocol Guide: XTT Assay for Cell Viability and Proliferation. Online. [Accessed 11 April 2024]. Available from: https://www.sigmaaldrich.com/LT/en/technical-documents/protocol/cell-culture-and-cell-culture-analysis/cell-counting-and-health-analysis/cell-proliferation-kit-xtt-assay?utm_source=google&utm_medium=cpc&utm_campaign=13896093114&utm_content=123561027814&gclid=Cj0KCQjwlN6wBhCcARIsAKZvD5iJdHuh-L9mjrpY7hSP0bxEQI83tgSAfwkr2HOlpQL676O1n_9ka6MaAnRaEALw_wcB
50. Cell Viability Assays | Thermo Fisher Scientific - LT. Online. [Accessed 11 April 2024]. Available from: https://www.thermofisher.com/lt/en/home/life-science/cell-analysis/cell-viability-and-regulation/cell-viability.html?gclid=Cj0KCQjwlN6wBhCcARIsAKZvD5g7eTk-k3I0QmoHmBc5ef35UsJBeJ9-8LumLYmx1GPCfiZWqGcywyIaAm98EALw_wcB&ef_id=Cj0KCQjwlN6wBhCcARIsAKZvD5g7eTk-k3I0QmoHmBc5ef35UsJBeJ9-8LumLYmx1GPCfiZWqGcywyIaAm98EALw_wcB:G:s&s_kwcid=AL!3652!3!655778876317!!!g!!!17329199729!147834142706&cid=bid_pca_frg_r01_co_cp1359_pjt0000_bid00000_0se_gaw_dy_pur_con&gad_source=1
51. HOWELL, Roger W., GODDU, S. Murty, NARRA, Venkat R., FISHER, Darrell R., SCHENTER, Robert E. and RAO, Dandamudi V. Radiotoxicity of gadolinium-148 and radium-223 in mouse testes: Relative biological effectiveness of alpha-particle emitters in vivo. *Radiation Research*. Online. 1997. Vol. 147, no. 3, p. 342–348. [Accessed 12 May 2024]. DOI 10.2307/3579342.